Electronic Supplementary Material (ESI) for Dalton Transactions.

Electronic Supplementary Information

for the manuscript entitled

Ruthenium complexes of phosphine-amide based ligands as efficient catalysts for transfer hydrogenation reactions

Samanta Yadav, Paranthaman Vijayan, Sunil Yadav and Rajeev Gupta*

Department of Chemistry, University of Delhi, Delhi 110007, India

E-mail: rgupta@chemistry.du.ac.in

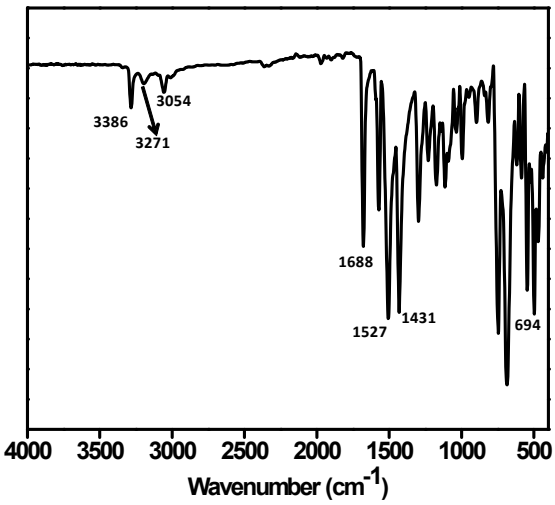

Figure S1. FTIR spectrum of ligand **HL[1]**.

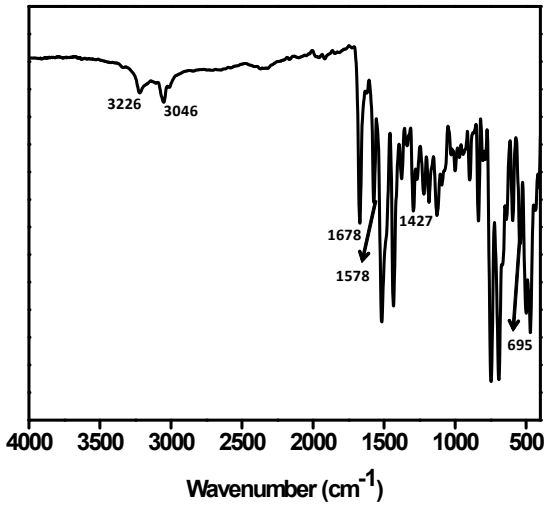

Figure S2. FTIR spectrum of ligand **HL[2]**.

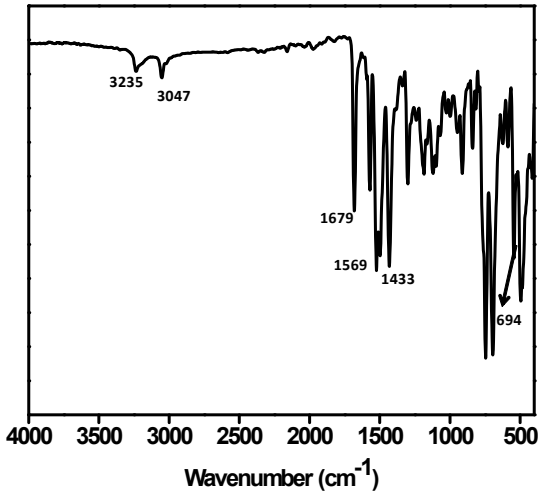

Figure S3. FTIR spectrum of ligand **HL**[3].

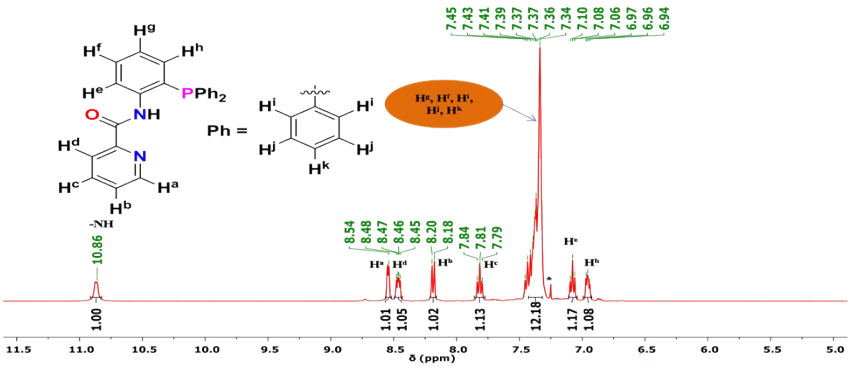

Figure S4. Selected part of ^{1}H NMR spectrum of ligand **HL**[1] in $CDCl_3$.

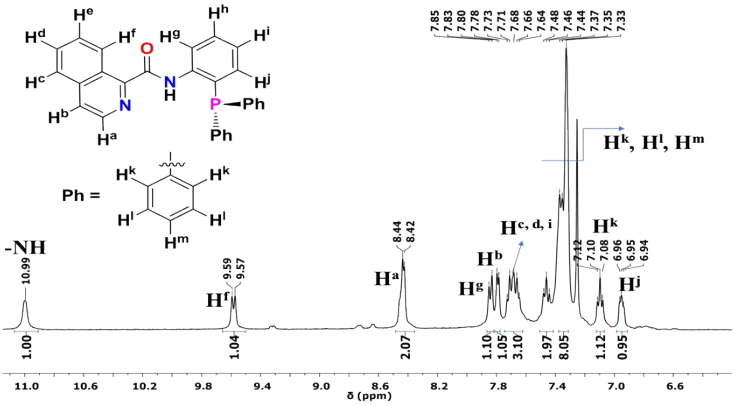

Figure S5. Selected part of ^{1}H NMR spectrum of ligand **HL**[2] in $CDCl_3$.

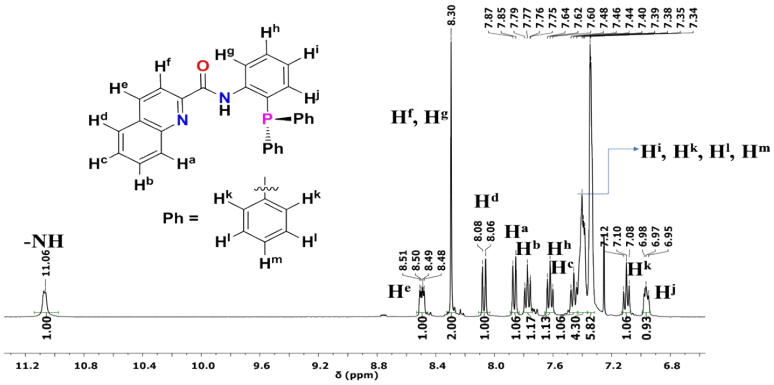

Figure S6. Selected part of ^{1}H NMR spectrum of ligand **HL^{3}** in $CDCl_3$.

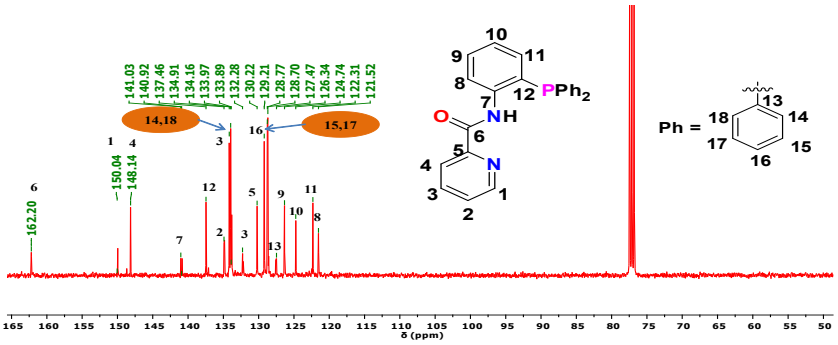

Figure S7. Selected part of ^{13}C NMR spectrum of ligand **HL^{1}** in $CDCl_3$.

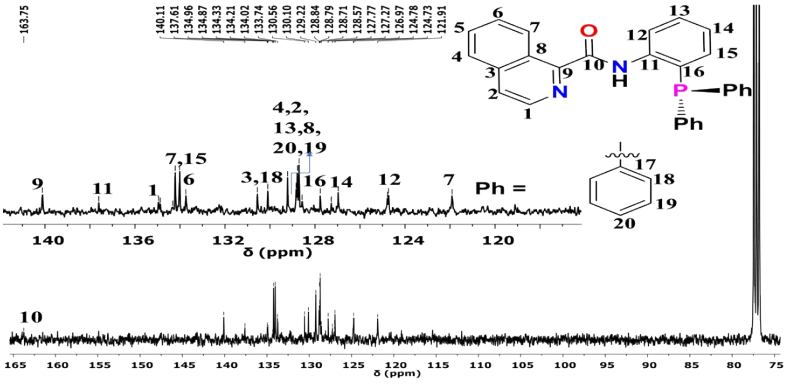

Figure S8. Selected part of ^{13}C NMR spectrum of ligand **HL^{2}** in $CDCl_3$.

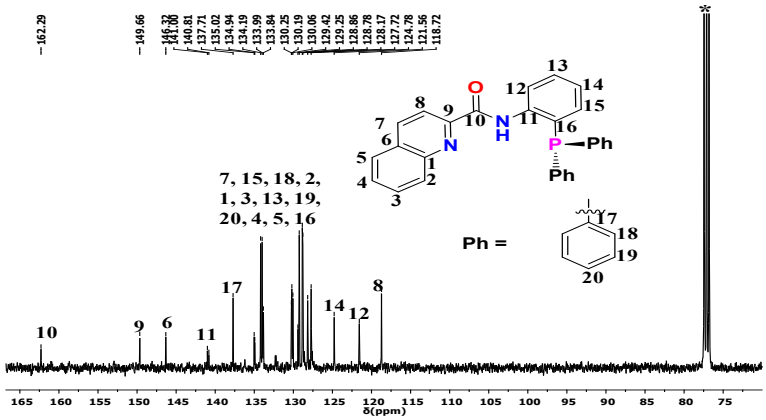

Figure S9. Selected part of ^{13}C NMR spectrum of ligand **HL^{3}** in $CDCl_3$.

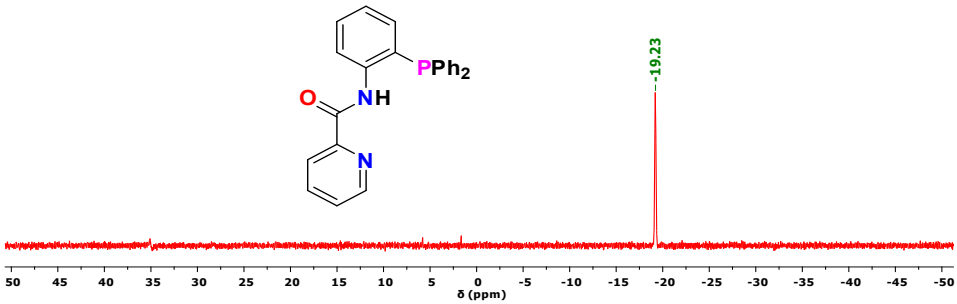

Figure S10. Selected part of ^{31}P NMR spectrum of ligand **HL^{1}** in $CDCl_3$.

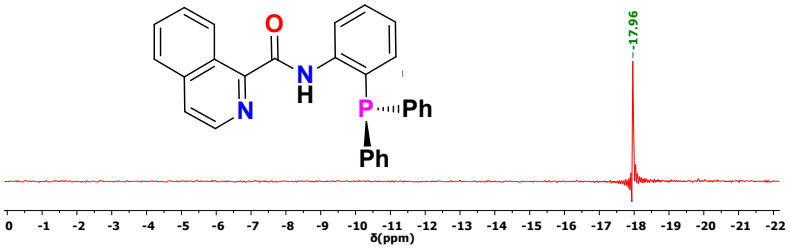

Figure S11. Selected part of ^{31}P NMR spectrum of ligand **HL^{2}** in $CDCl_3$.

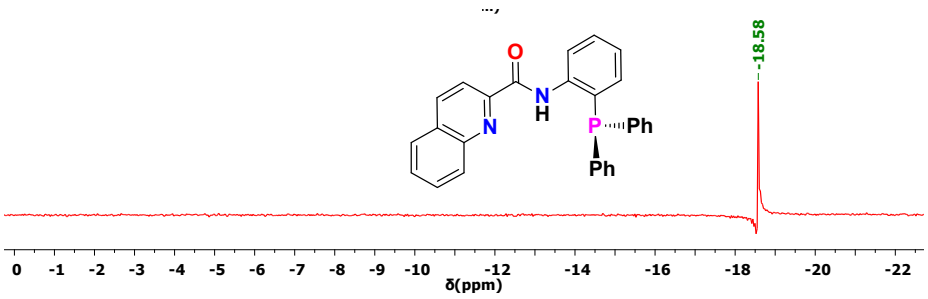

Figure S12. Selected part of ^{31}P NMR spectrum of ligand **HL³** in $CDCl_3$.

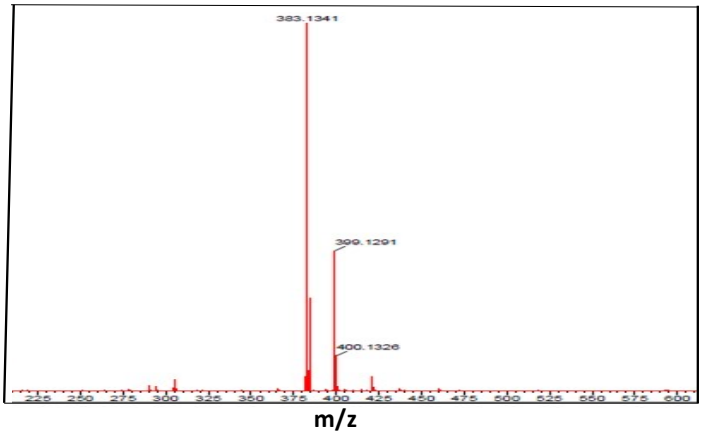

Figure 13. ESI^+-MS spectrum of ligand **HL¹** in MeOH.

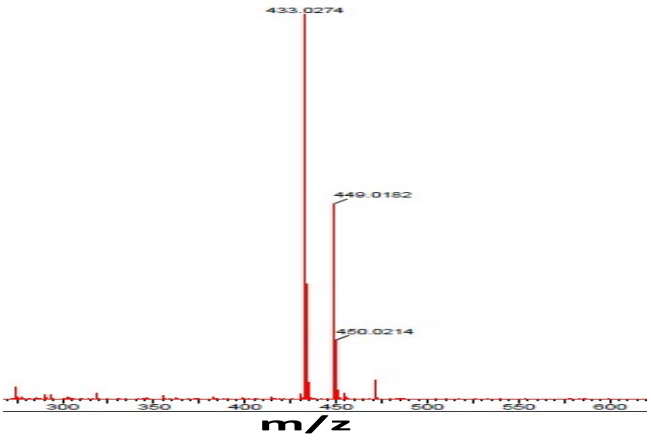

Figure 14. ESI^+-MS spectrum of ligand **HL²** in MeOH.

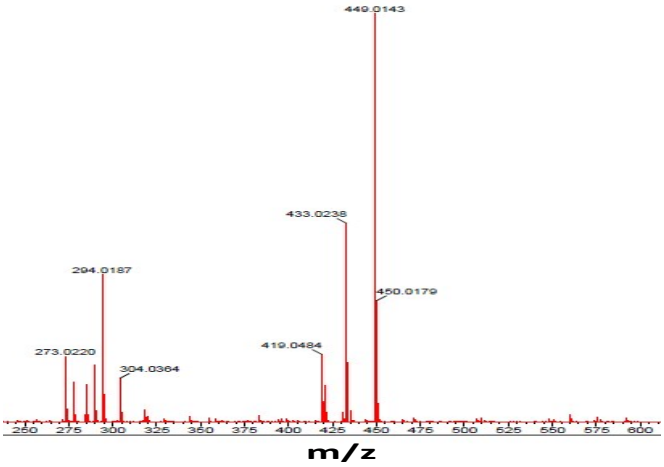

Figure 15. ESI^{+}-MS spectrum of ligand **HL^{3}** in MeOH.

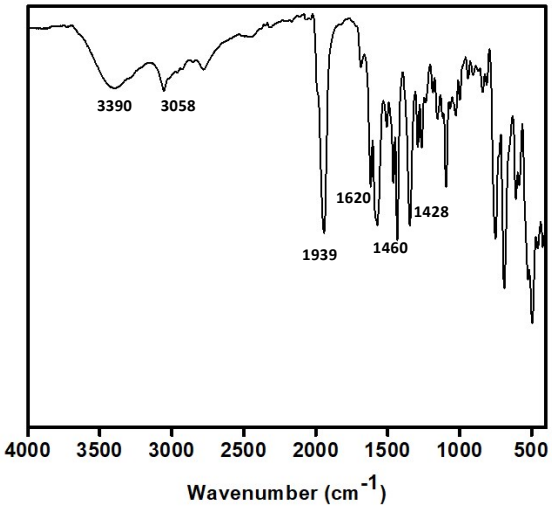

Figure S16. FTIR spectrum of complex **1**.

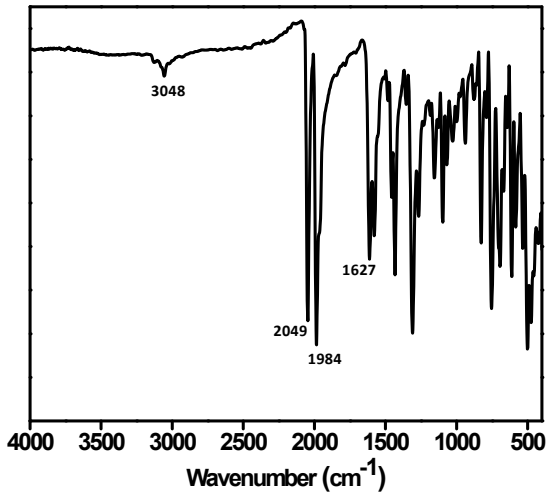

Figure S17. FTIR spectrum of complex **2**.

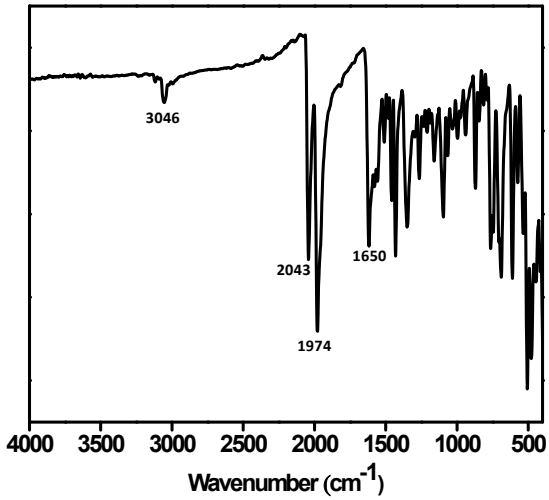

Figure S18. FTIR spectrum of complex **3**.

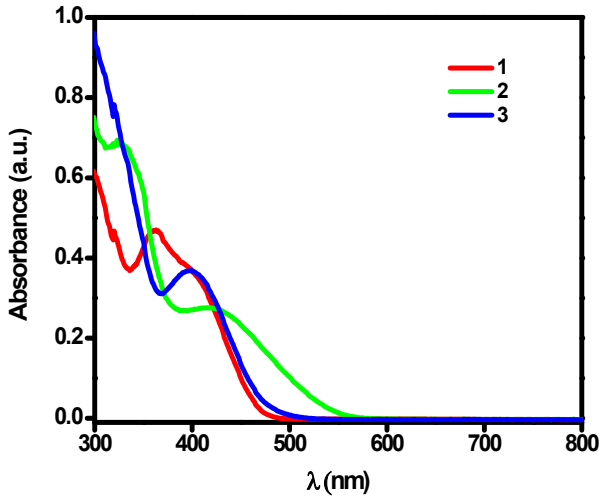

Figure S19. UV-Vis spectra of complexes **1-3** recorded in DMF.

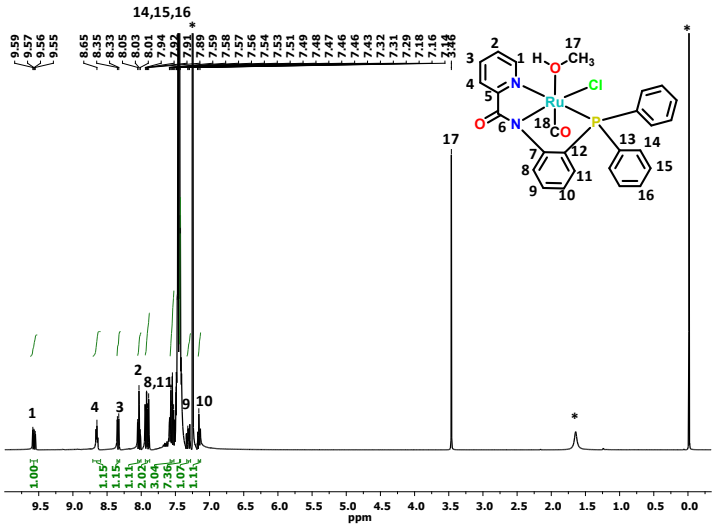

Figure S20. ^{1}H NMR spectrum of complex **1** in $CDCl_3$.* Represents residual solvent peak.

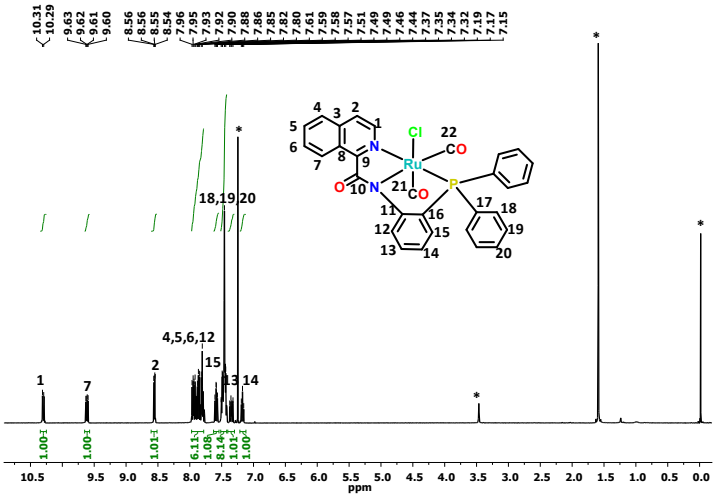

Figure S21. ^{1}H NMR spectrum of complex **2** in $CDCl_3$.* Represents residual solvent peak.

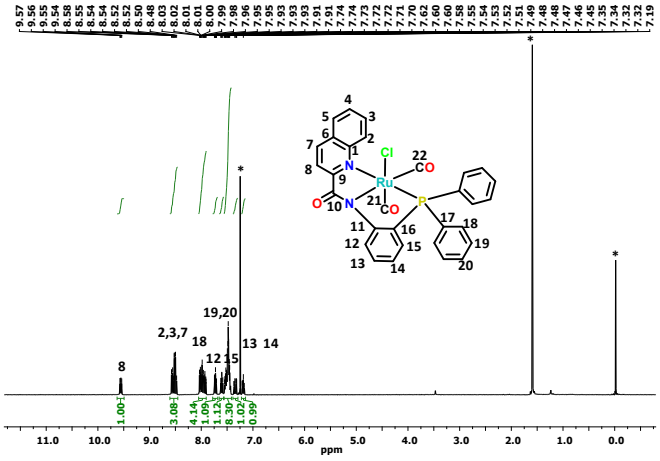

Figure S22. ^{1}H NMR spectrum of complex **3** in $CDCl_3$.* Represents residual solvent peak.

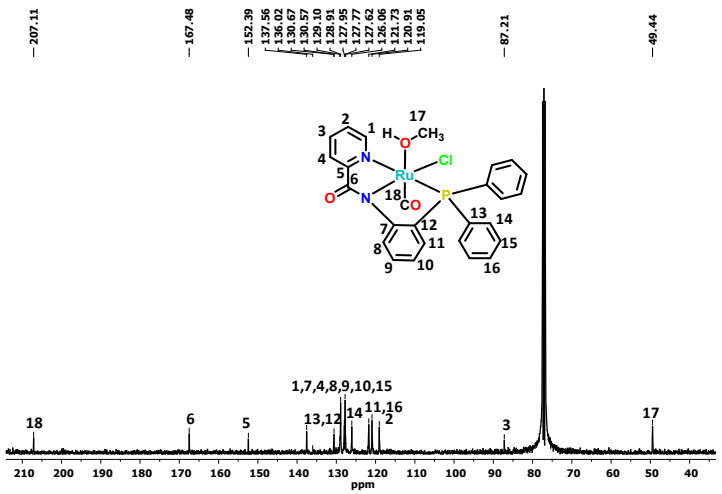

Figure S23. Selected part of ^{13}C NMR spectrum of complex **1** in $CDCl_3$.* Represents residual solvent peak.

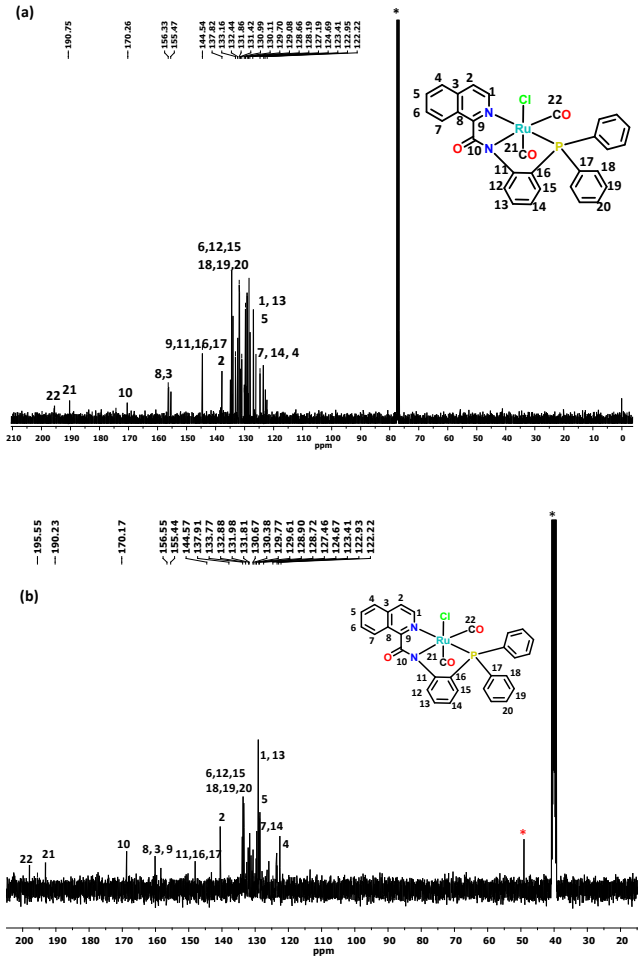

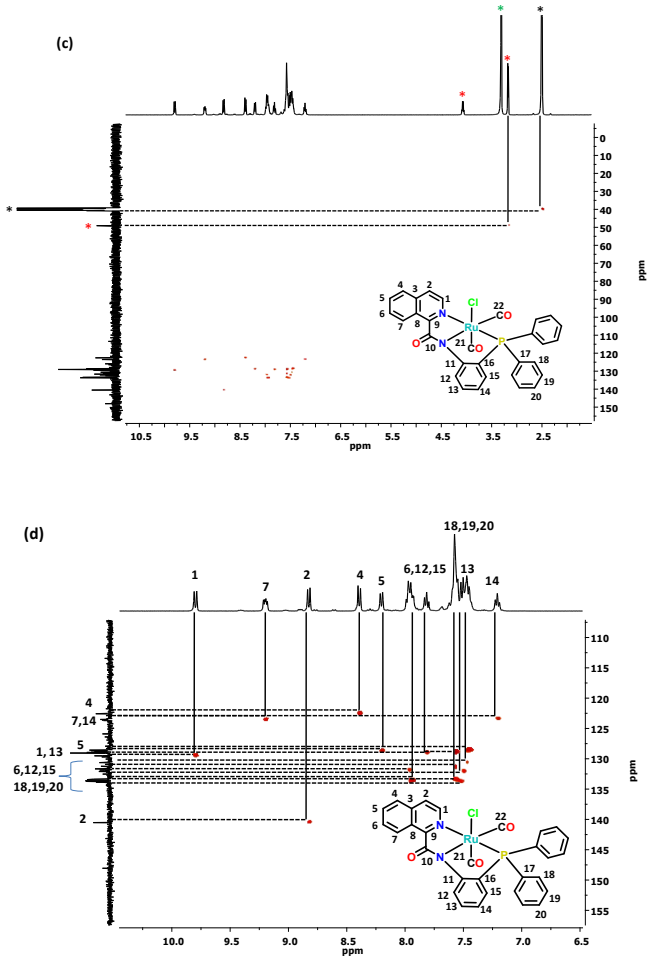

Figure S24. (a) Selected part of ^{13}C NMR spectrum of complex **2** in $CDCl_3$. (b) ^{13}C NMR spectrum of complex **2** in DMSO-d_6. (c) HSQC spectrum of complex **2** in DMSO-d_6. (d) Expansion of HSQC signals in the range of 6.6 to 10.0 ppm for ^{1}H NMR spectrum and 120-155 ppm for ^{13}C NMR spectrum. Black, red and green asterisks represent the NMR solvent and residual solvents methanol and adventitious H_2O, respectively.

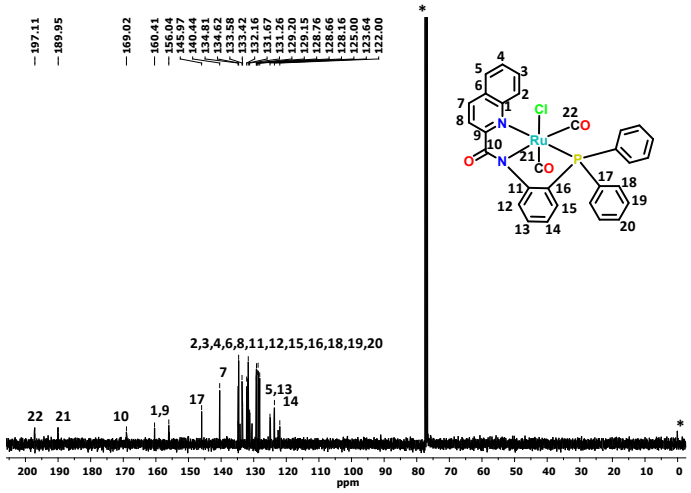

Figure S25. Selected part of ^{13}C NMR spectrum of complex **3** in $CDCl_3$.* Represents residual solvent peak.

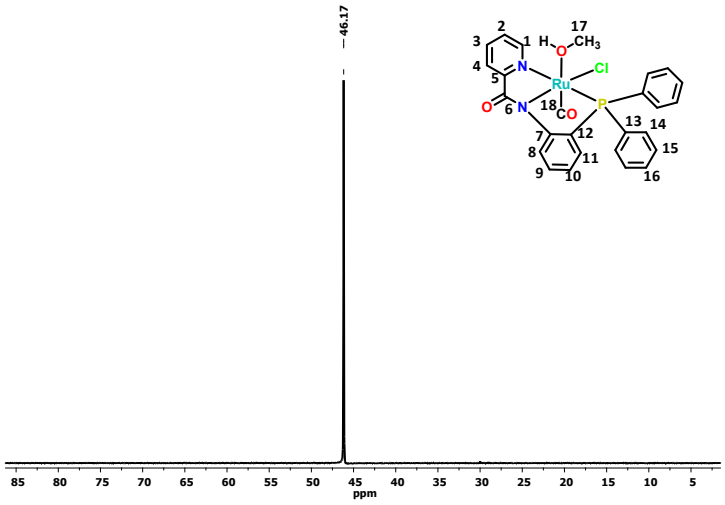

Figure S26. Selected part of ^{31}P NMR spectrum of complex **1** in $CDCl_3$.

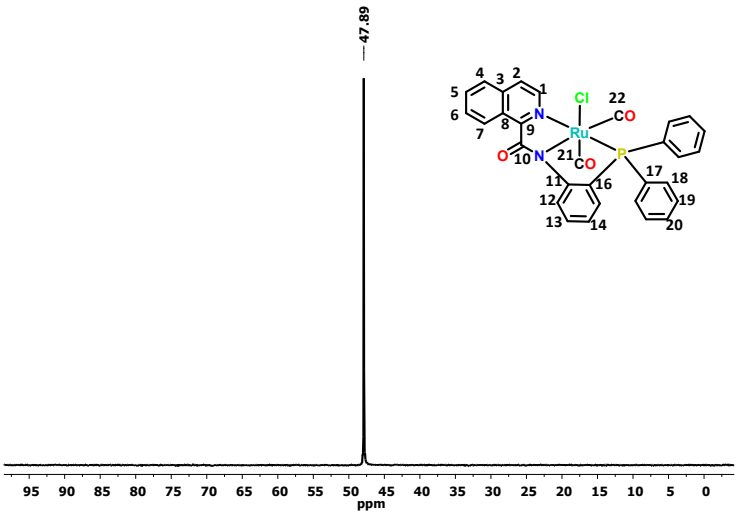

Figure S27. Selected part of ^{31}P NMR spectrum of complex **2** in $CDCl_3$.

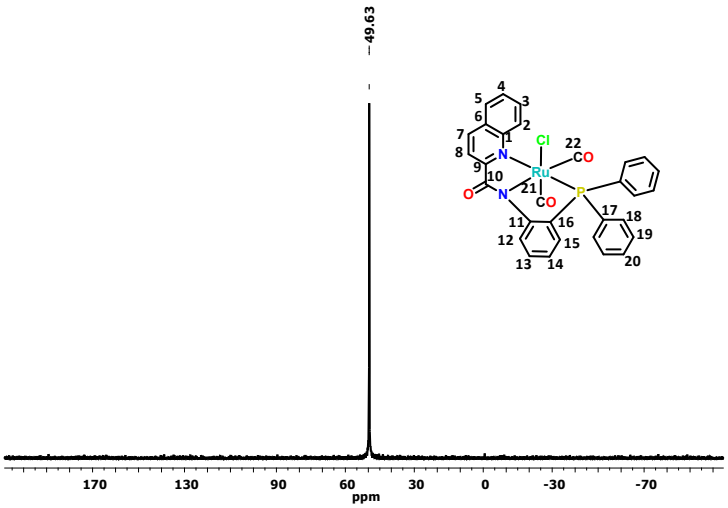

Figure S28. Selected part of ^{31}P NMR spectrum of complex **3** in $CDCl_3$.

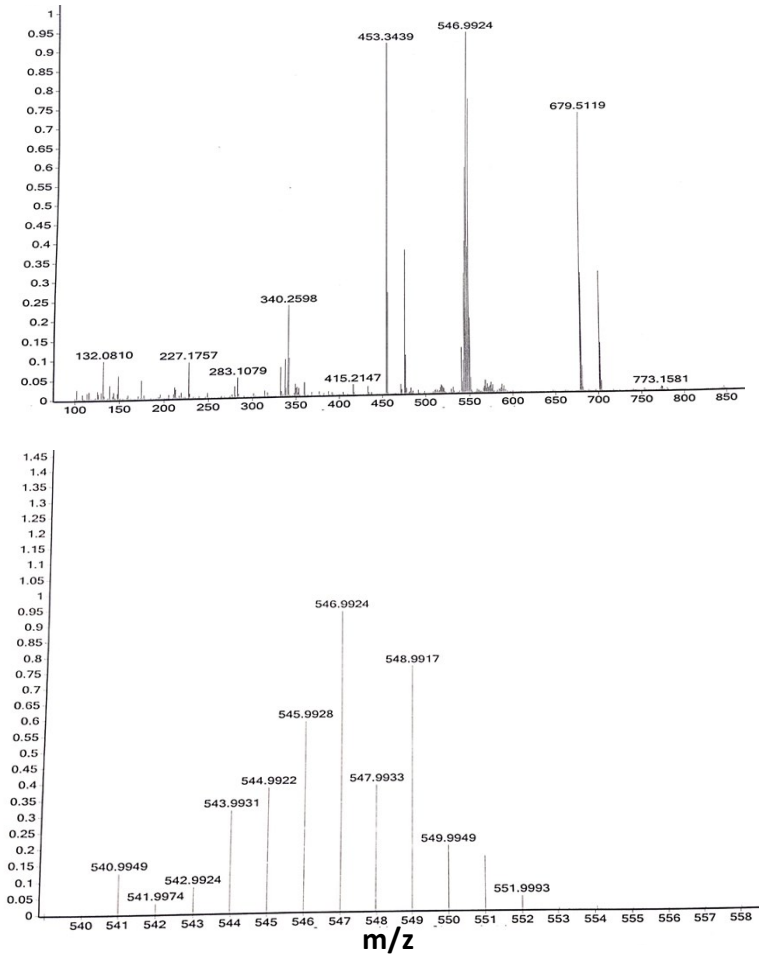

Figure S29. ESI$^+$-MS spectrum of complex **1** in MeOH.

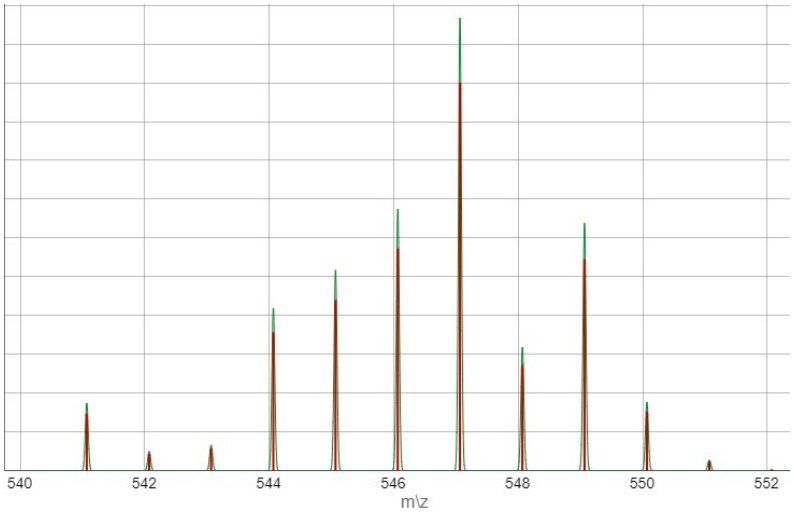

Figure S30. Experimental (green) and simulated (red) pattern for molecular ion peak at *m/z* = 547.0647 $[M–CH_3OH]+H]^+$ for complex **1**.

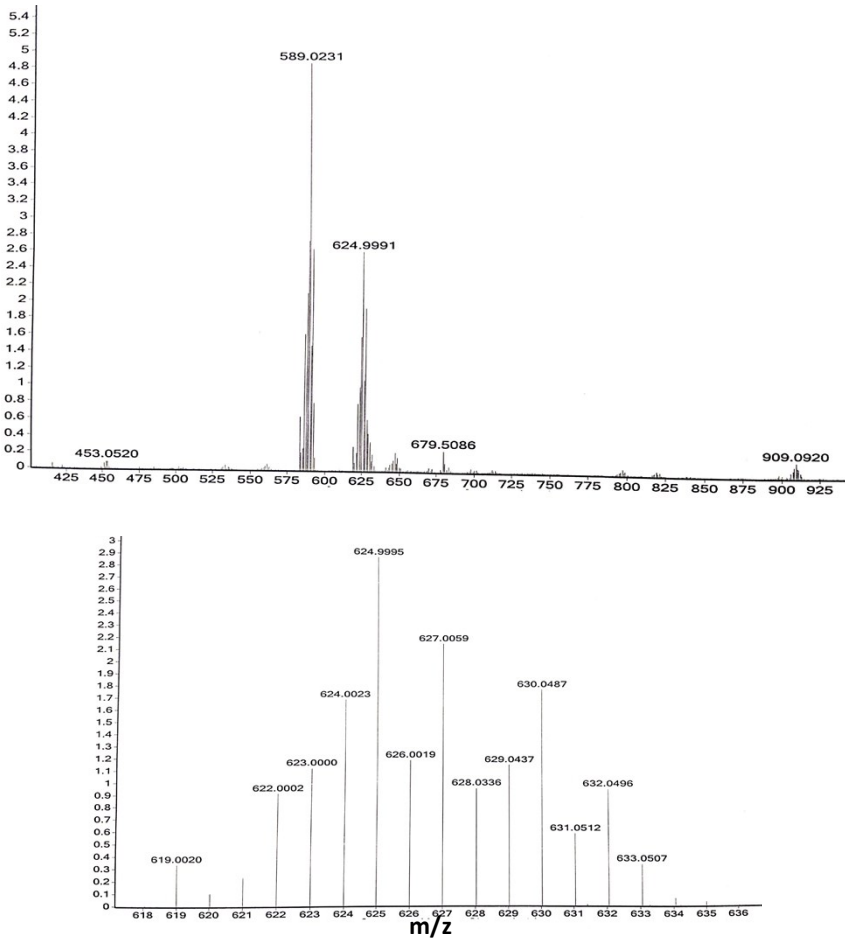

Figure S31. ESI$^+$-MS spectrum of complex **2** in MeOH.

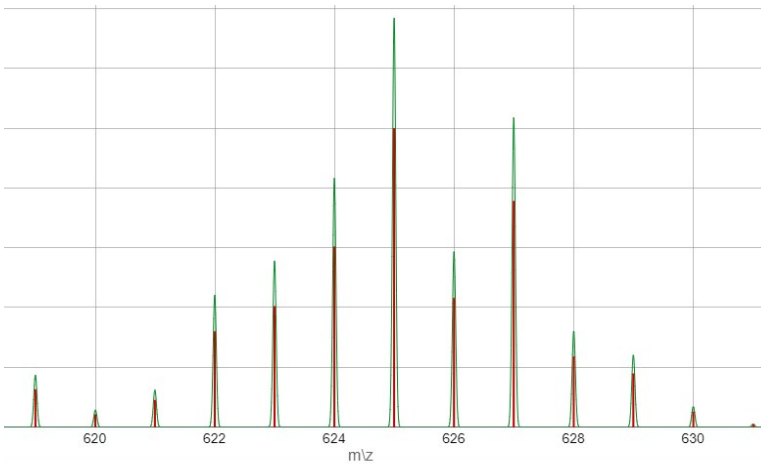

Figure S32. Experimental (green) and simulated (red) pattern for molecular ion peak at *m/z* = 625.002 $[M+H]^+$for complex **2**.

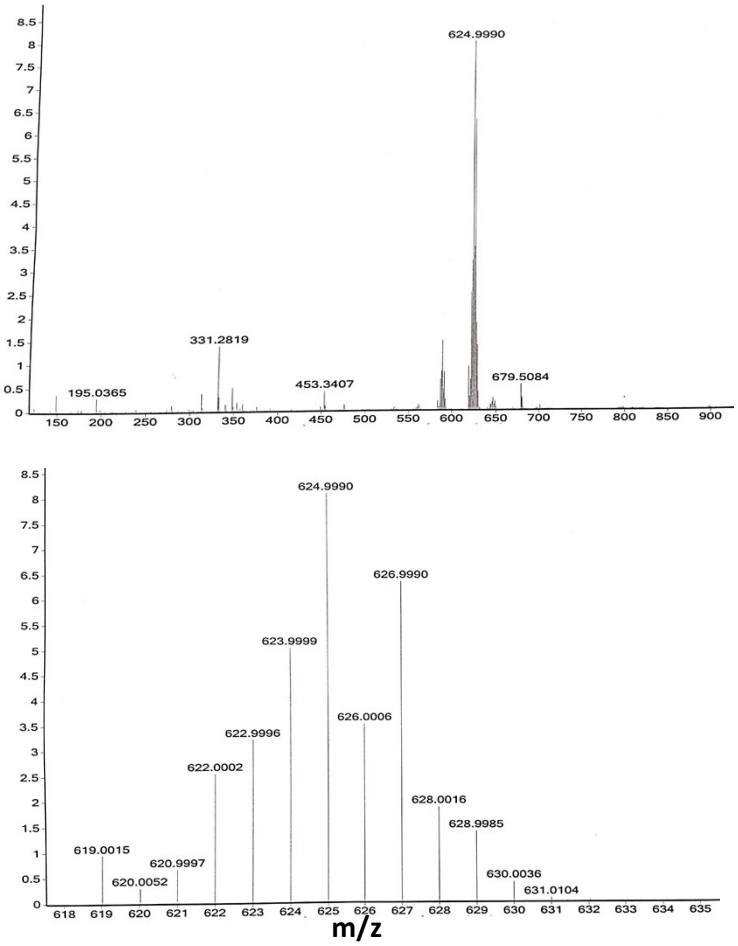

Figure S33. ESI$^+$-MS spectrum of complex **3**.

Figure S34. Experimental (green) and simulated (red) pattern for molecular ion peak at *m/z* = 625.0021 $[M+H]^+$ for complex **3**.

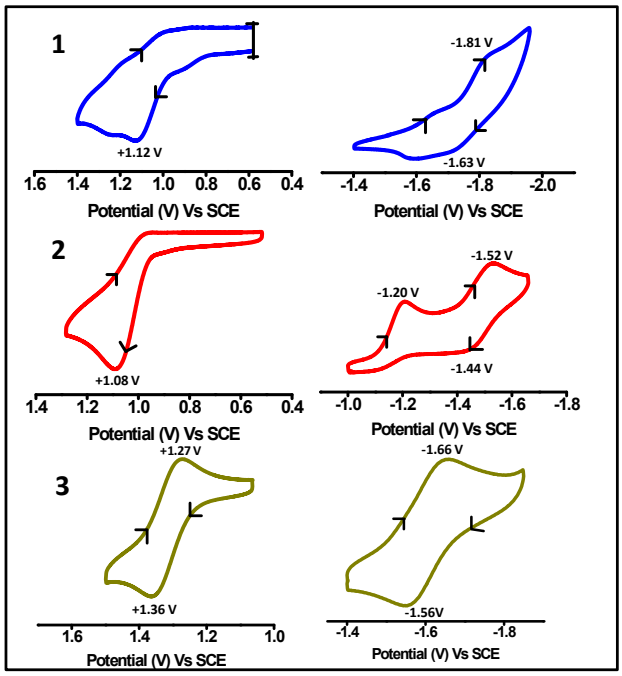

Figure S35. Cyclic voltammograms of complexes **1–3**. Conditions: Solvent, CH_3OH; complex, ca. 1 mM; supporting electrolyte, TBAP, ca. 100 mM; working electrode, glassy carbon; reference electrode, Ag/Ag^+; auxiliary electrode, Pt wire; scan rate, 100 mV/s.

Gas chromatograms for various organic products with the method used:

Method A: Column information: Elite-5, L=30 m, ID: 0.25 mm; injector temperature: 50°C; column flow rate: 1.13 mL/min; column temperature: 50-180 °C; temperature program: 10 °C/min; detector temperature: 250 °C

Method B: Column information: Elite-5, L=30 m, ID: 0.25 mm; injector temperature: 100°C; column flow rate: 1.13 mL/min; column temperature: 80-180 °C; temperature program: 8 °C/min; detector temperature: 270 °C

Method C: Column information: Rtx-5, L = 30 m, ID: 0.25 mm; injector temperature: 220 °C; column flow rate: 1.13 mL/min; column temperature: 100 – 180 °C; temperature program: 6 °C/min; detector temperature: 250 °C.

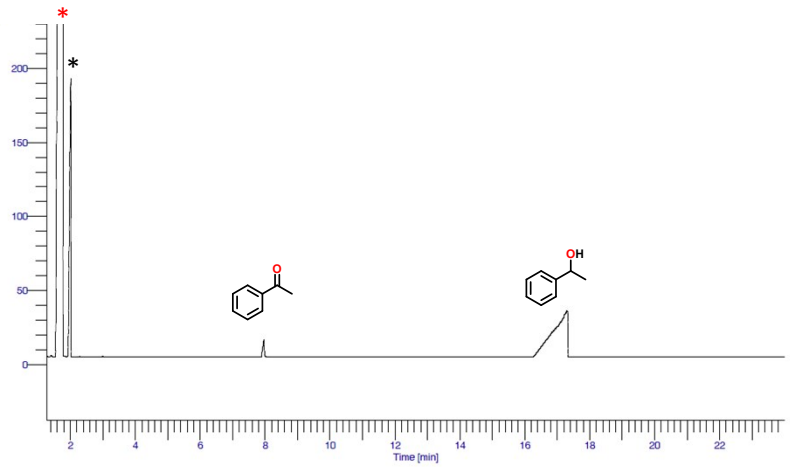

Figure S36. Gas chromatogram for the transfer hydrogenation of acetophenone (Table 2, Entry 1) using method A. * Represents ethyl acetate and * represents isopropanol.

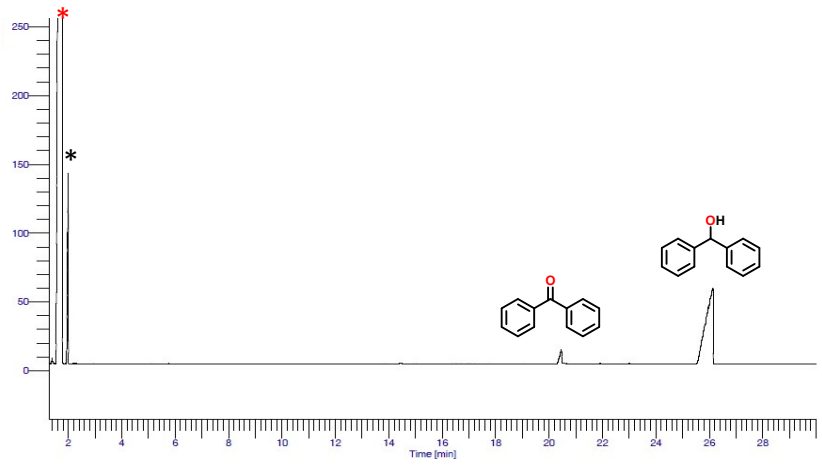

Figure S37. Gas chromatogram for the transfer hydrogenation of benzophenone, Table 2, Entry 2 using method A. * Represents ethyl acetate and * represents isopropanol.

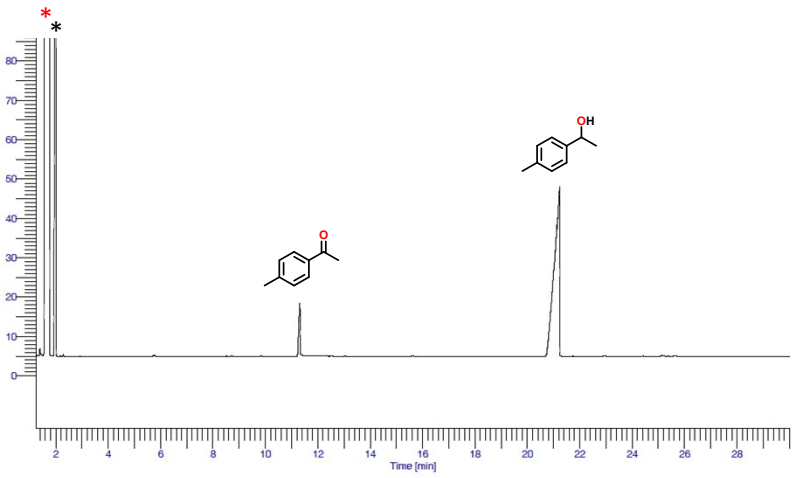

Figure S38. Gas chromatogram for the transfer hydrogenation of 4-methylacetophenone, Table 2, Entry 3 using method A. * Represents ethyl acetate and * represents isopropanol.

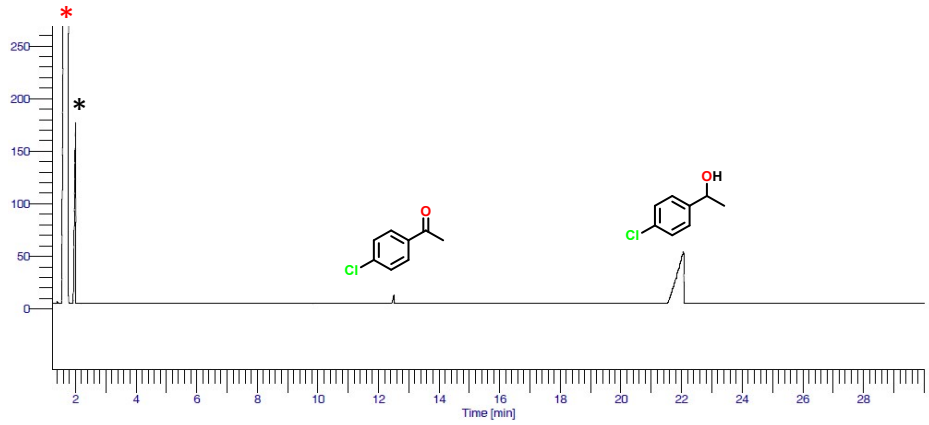

Figure S39. Gas chromatogram for the transfer hydrogenation of 4-chloroacetophenone, Table 2, Entry 4 using method A. * Represents ethyl acetate and * represents isopropanol.

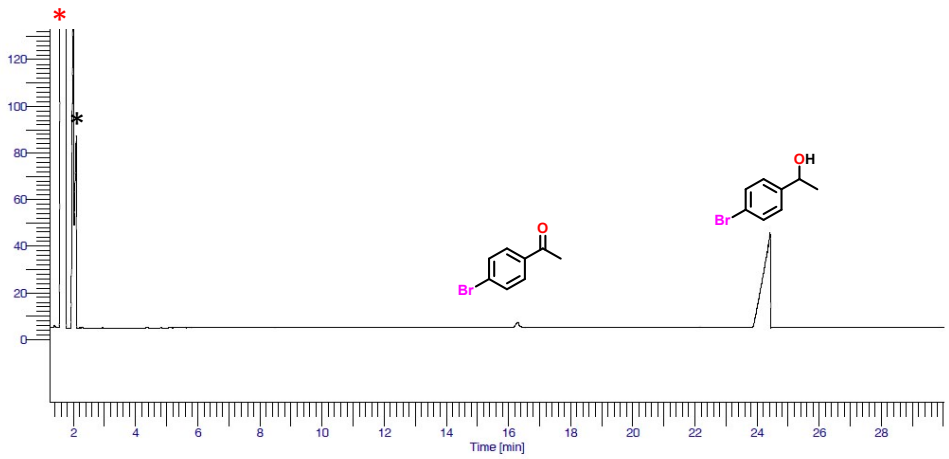

Figure S40. Gas chromatogram for the transfer hydrogenation of 4-bromoacetophenone, Table 2, Entry 5 using method A. * Represents ethyl acetate and * represents isopropanol.

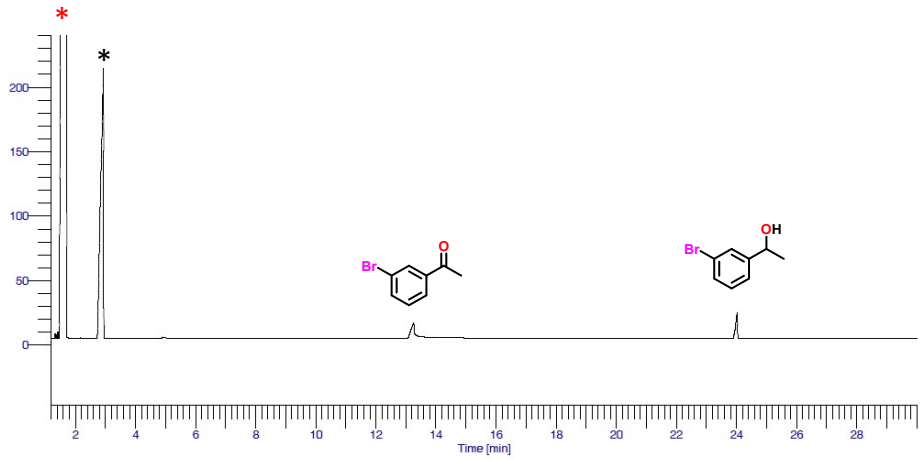

Figure S41. Gas chromatogram for the transfer hydrogenation of 3-bromoacetophenone, Table 2, Entry 6 using method B. * Represents ethyl acetate and * represents isopropanol.

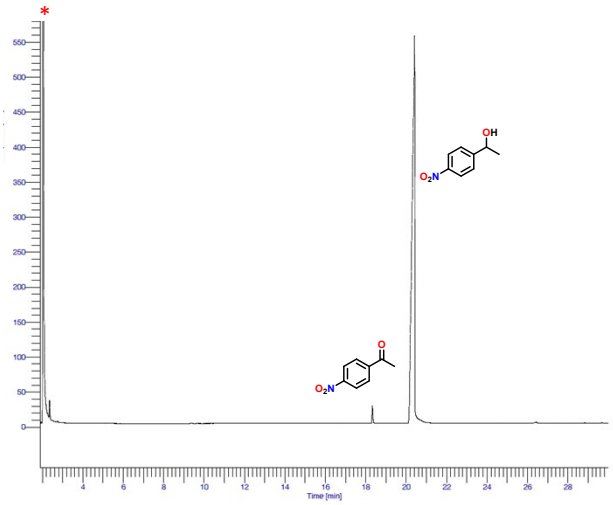

Figure S42. Gas chromatogram for the transfer hydrogenation of 4-nitroacetophenone, Table 2, Entry 7 using method A. * Represents ethyl acetate.

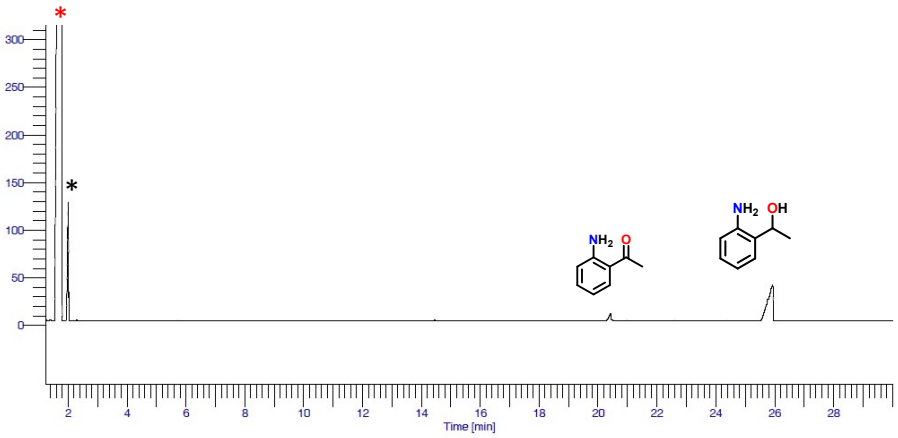

Figure S43. Gas chromatogram for the transfer hydrogenation of 2-aminoacetophenone, Table 2, Entry 8 using method A. * Represents ethyl acetate and * represents isopropanol.

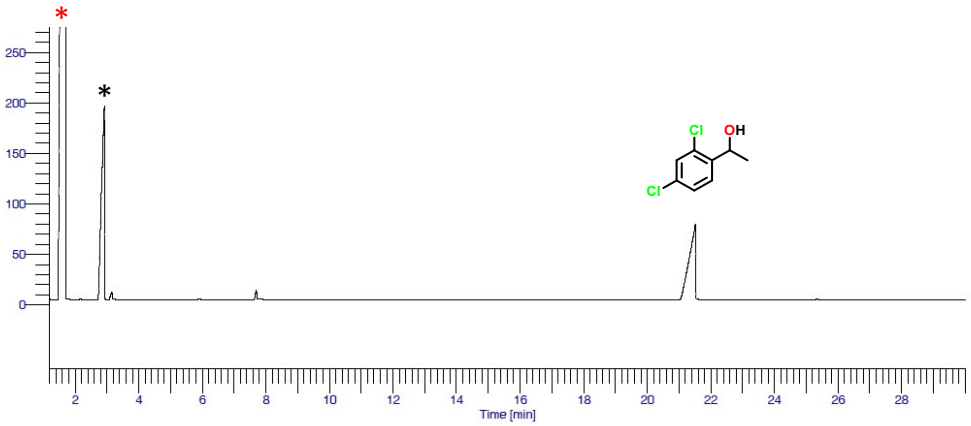

Figure S44. Gas chromatogram for the transfer hydrogenation of 2,4-dichloroacetophenone, Table 2, Entry 9 using method B. * Represents ethyl acetate and * represents isopropanol.

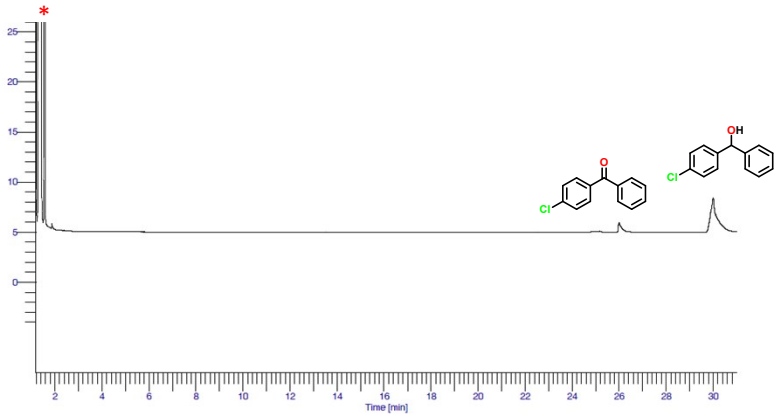

Figure S45. Gas chromatogram for the transfer hydrogenation of 4-chlorobenzophenone, Table 2, Entry 10 using method A. * Represents ethyl acetate.

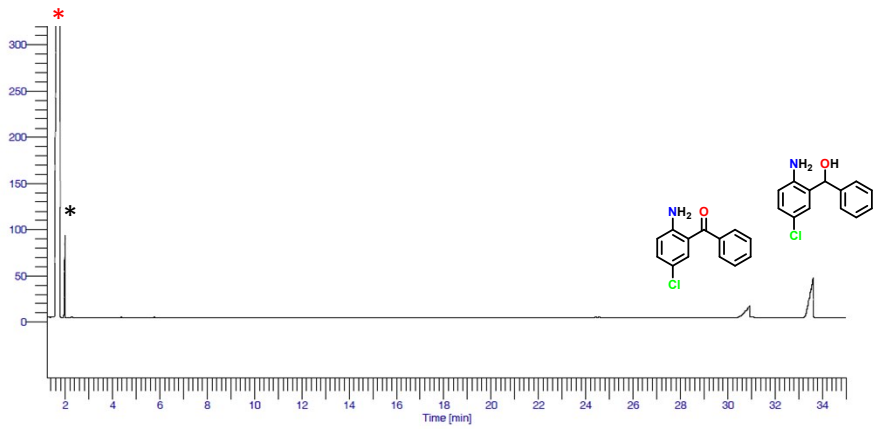

Figure S46. Gas chromatogram for the transfer hydrogenation of 2-amino-4-chlorobenzophenone, Table 2, Entry 11 using method A. * Represents ethyl acetate and * represents isopropanol.

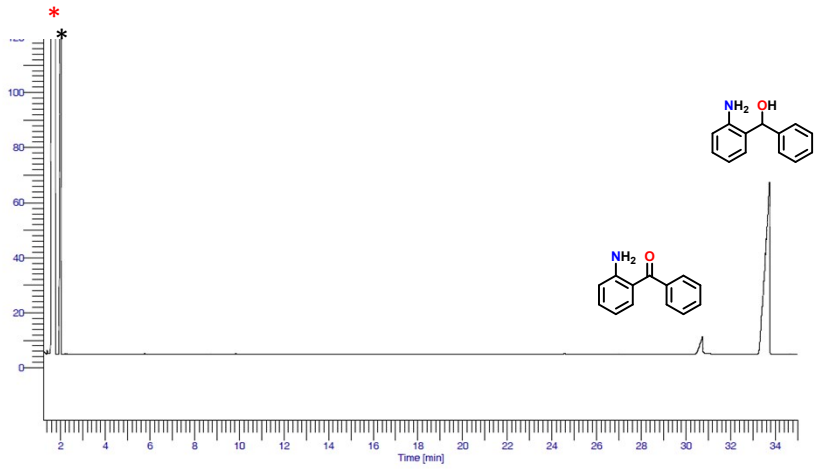

Figure S47. Gas chromatogram for the transfer hydrogenation of 2-aminobenzophenone, Table 2, Entry 12 using method A. * Represents ethyl acetate and * represents isopropanol.

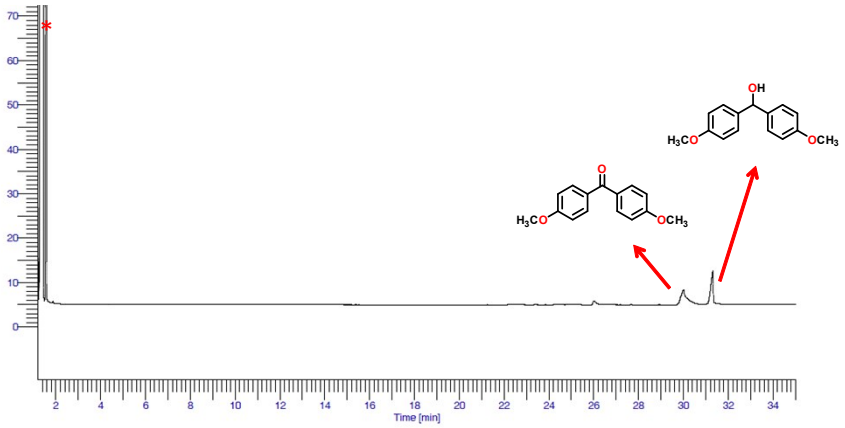

Figure S48. Gas chromatogram for the transfer hydrogenation of 4,4'-dimethoxybenzophenone, Table 2, Entry 13 using method B. * Represents ethyl acetate.

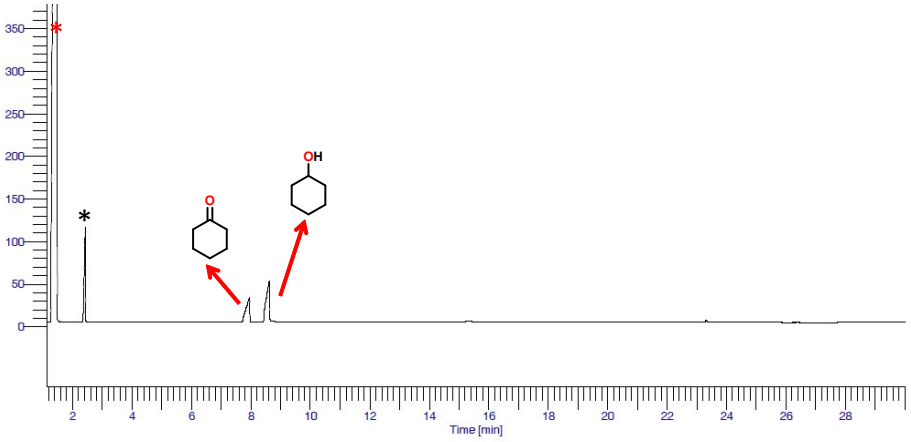

Figure S49. Gas chromatogram for the transfer hydrogenation of cyclohexanone, Table 2, Entry 14 using method B. * Represents ethyl acetate and * represents isopropanol.

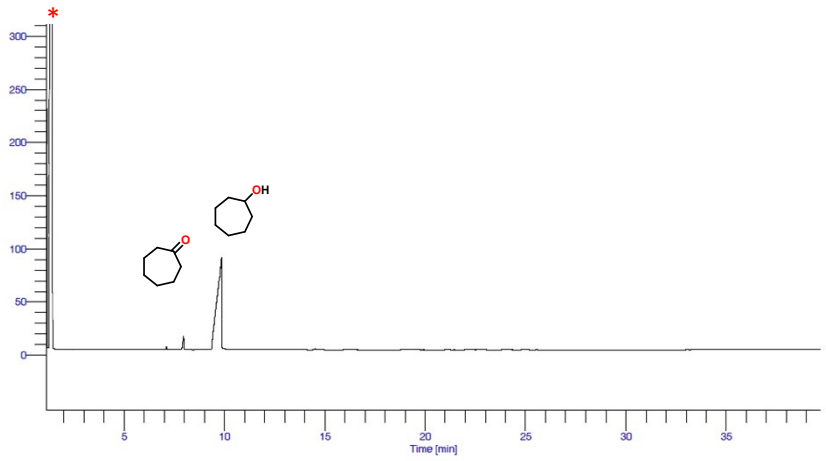

Figure S50. Gas chromatogram for the transfer hydrogenation of cycloheptanone, Table 2, Entry 15 using method A. * Represents ethyl acetate.

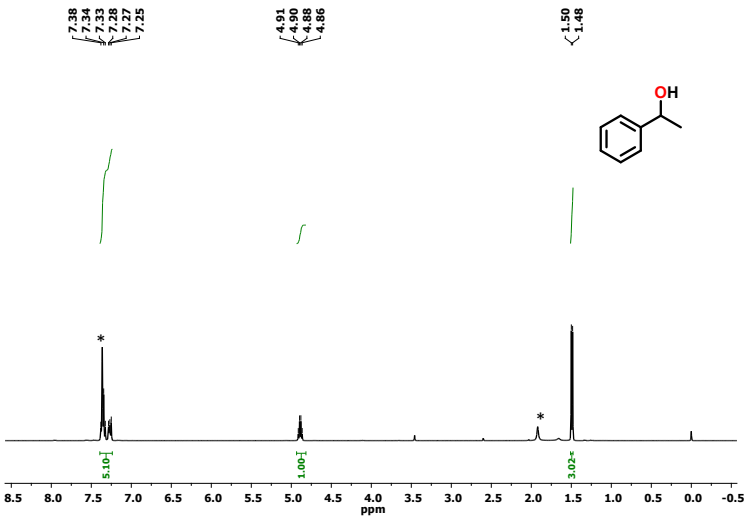

Figure S51. ^{1}H NMR spectrum of product **1** in $CDCl_3$. * Represents the residual solvent peak and/or water.

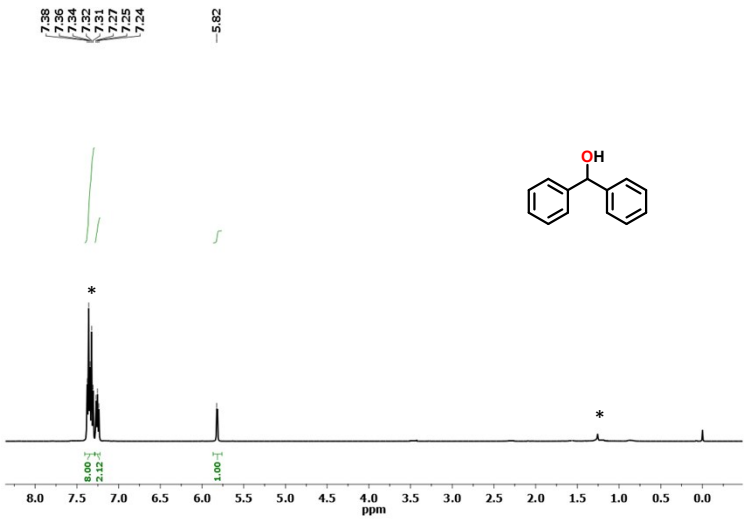

Figure S52. ^{1}H NMR spectrum of product **2** in $CDCl_3$. * Represents the residual solvent peak and/or water.

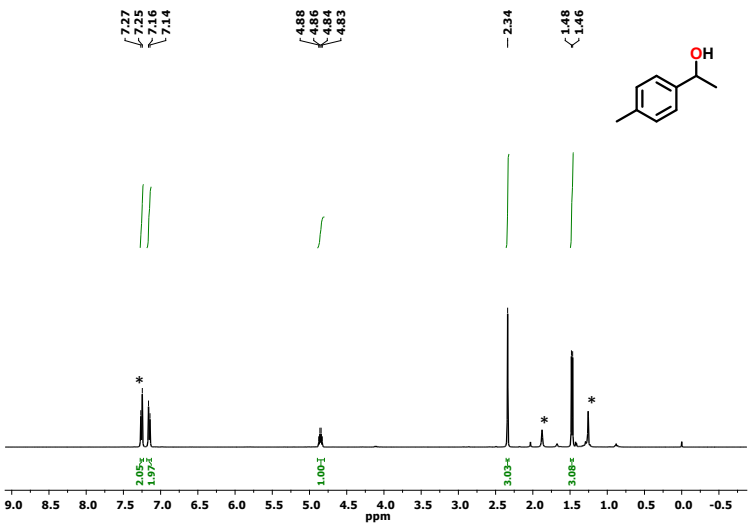

Figure S53. ^{1}H NMR spectrum of product **3** in $CDCl_3$. * Represents the residual solvent peak and/or water.

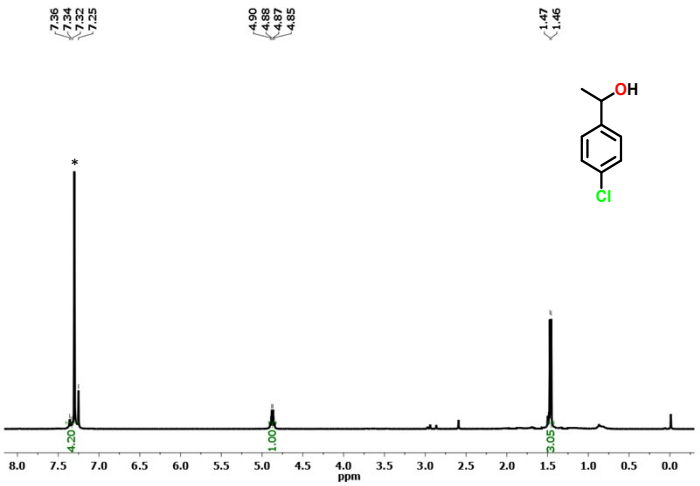

Figure S54. ^{1}H NMR spectrum of product **4** in $CDCl_3$. * Represents the residual solvent peak.

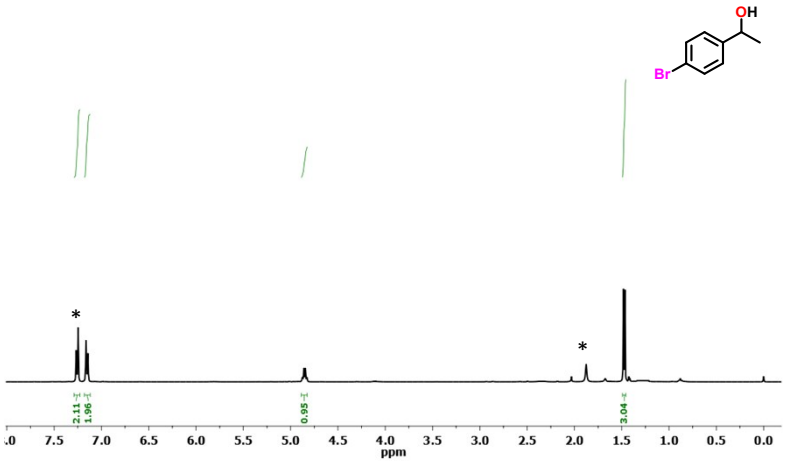

Figure S55. ^{1}H NMR spectrum of product **5** in $CDCl_3$.* Represents the residual solvent peak and/or water.

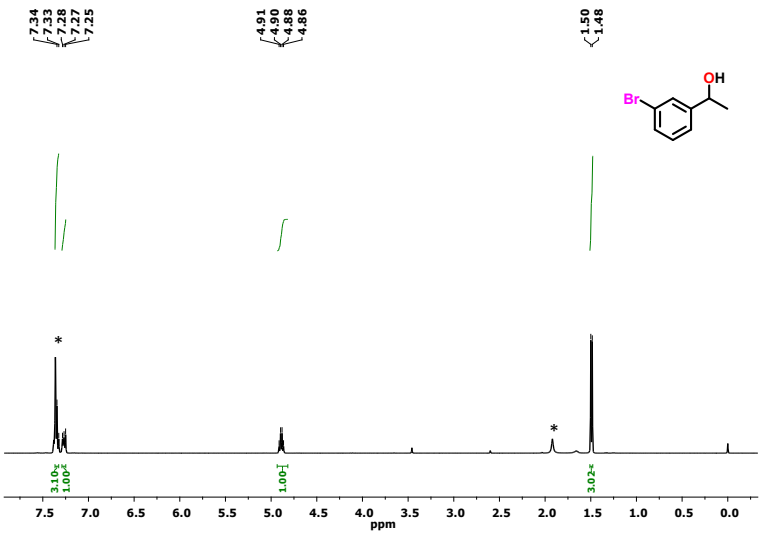

Figure S56. ^{1}H NMR spectrum of product **6** in $CDCl_3$. * Represents the residual solvent peak and/or water.

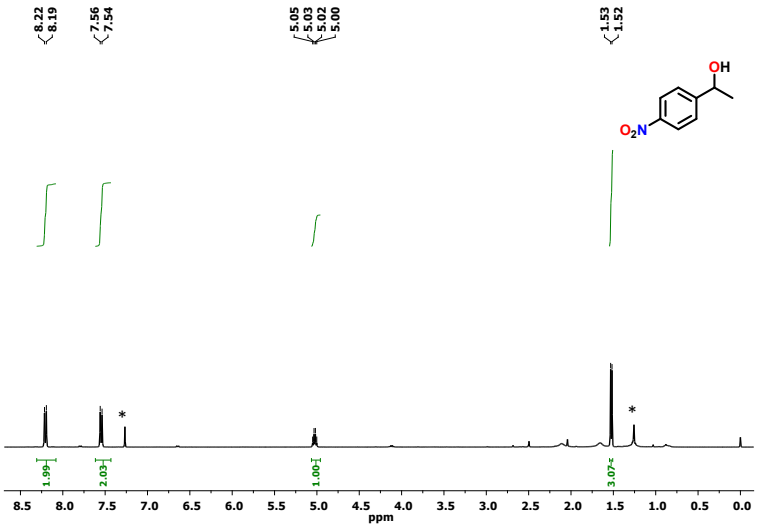

Figure S57. ^{1}H NMR spectrum of product **7** in $CDCl_3$. * Represents the residual solvent peak and/or water.

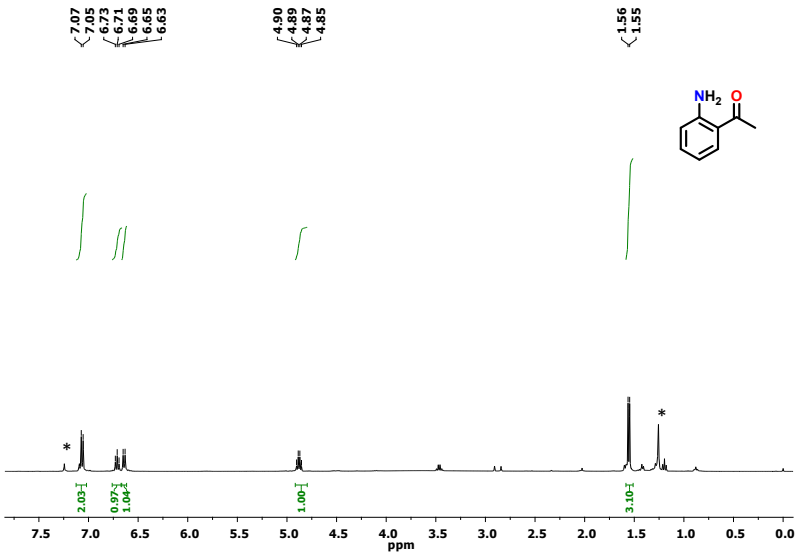

Figure S58. ^{1}H NMR spectrum of product **8** in $CDCl_3$. * Represents the residual solvent peak and/or water.

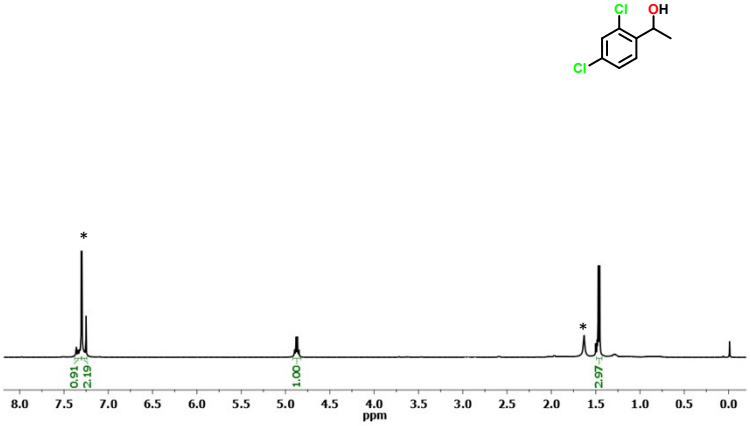

Figure S59. ^{1}H NMR spectrum of compound **9** in $CDCl_3$. * Represents the residual solvent peak and/or water.

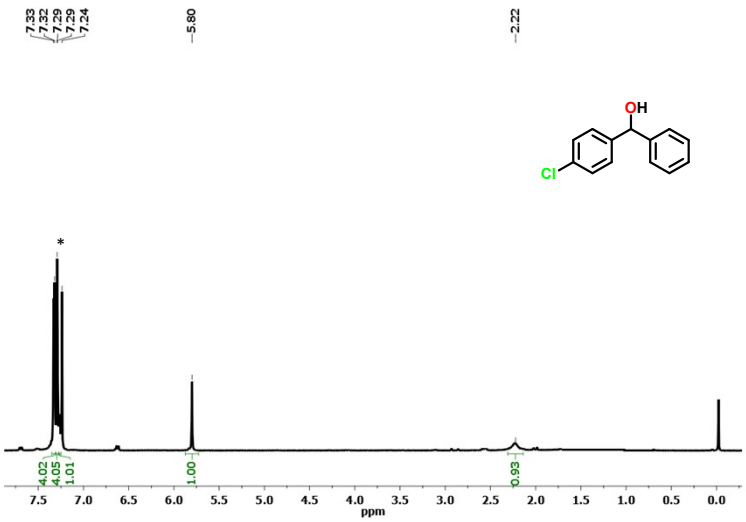

Figure S60. ^{1}H NMR spectrum of compound **10** in $CDCl_3$. * Represents the residual solvent peak and/or water.

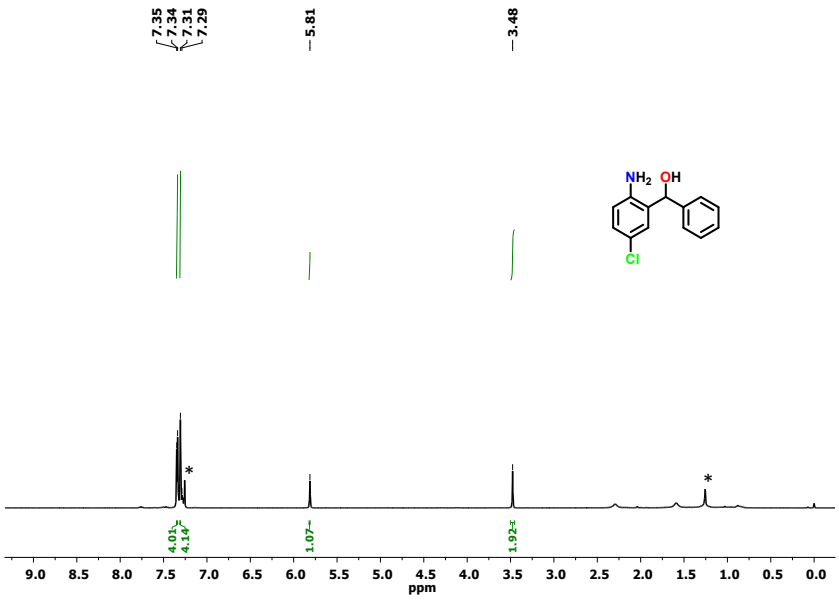

Figure S61. ^{1}H NMR spectrum of compound **11** in $CDCl_3$. * Represents the residual solvent peak and/or water.

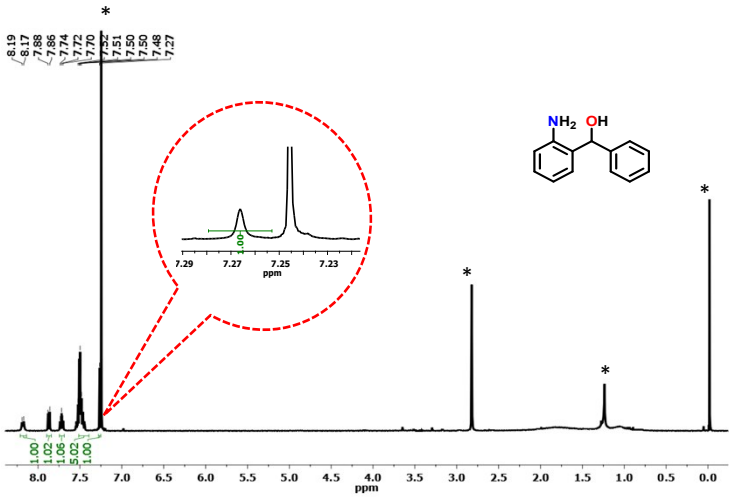

Figure S62. ^{1}H NMR spectrum of compound **12** in $CDCl_3$. * Represents the residual solvent peak and/or water.

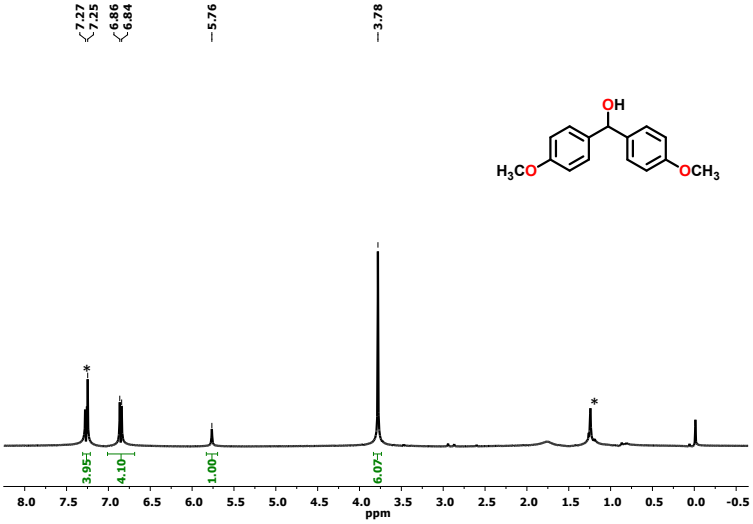

Figure S63. ^{1}H NMR spectrum of compound **13** in $CDCl_3$. * Represents the residual solvent peak and/or water.

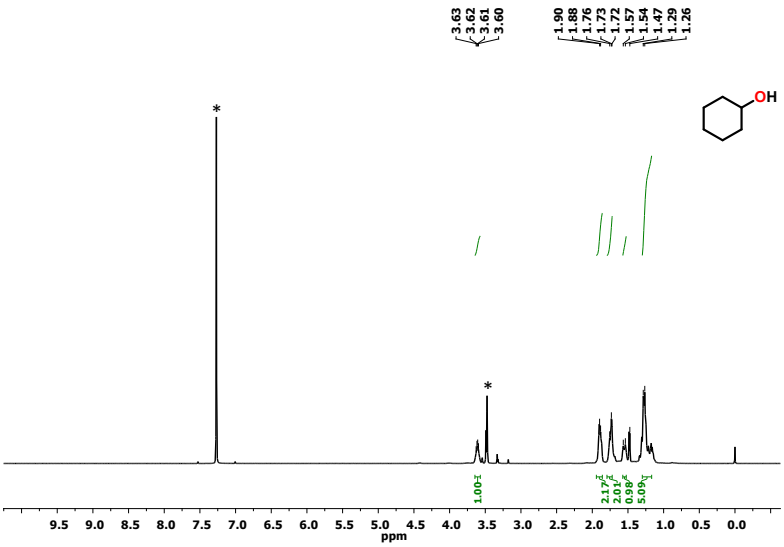

Figure S64. ^{1}H NMR spectrum of product **14** in $CDCl_3$. * Represents the residual solvent peak and/or water.

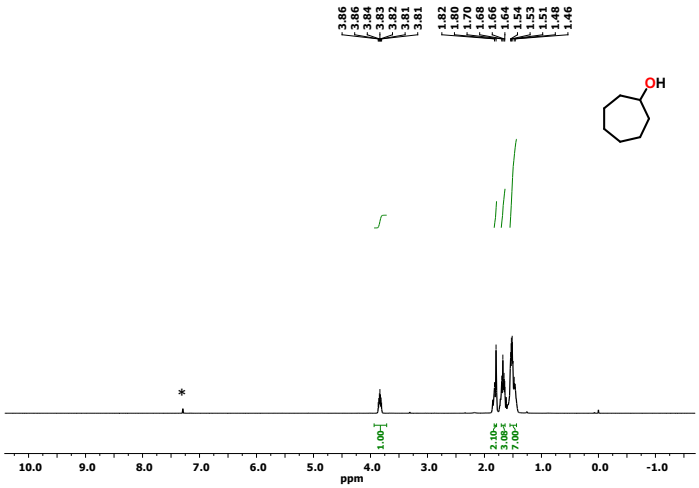

Figure S65. ^{1}H NMR spectrum of product **15** in $CDCl_3$. * Represents the residual solvent peak and/or water.

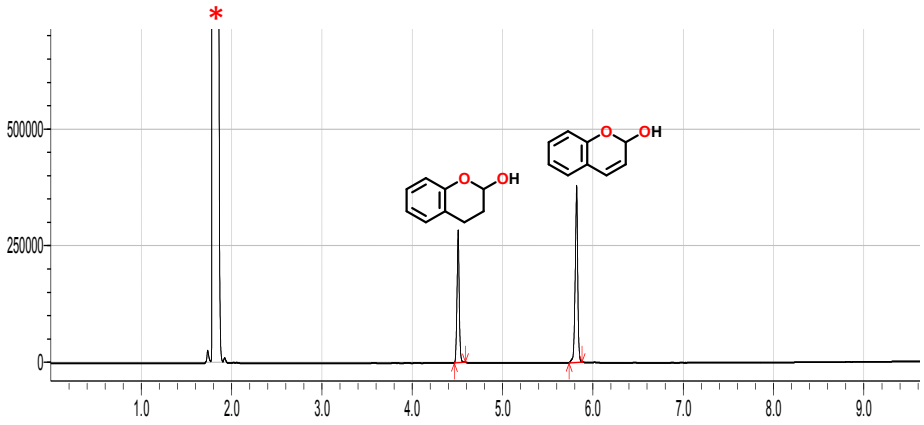

Figure S66. Gas chromatogram for the transfer hydrogenation of coumarin, Scheme 2, Entry 1 using method C. * Represents ethyl acetate.

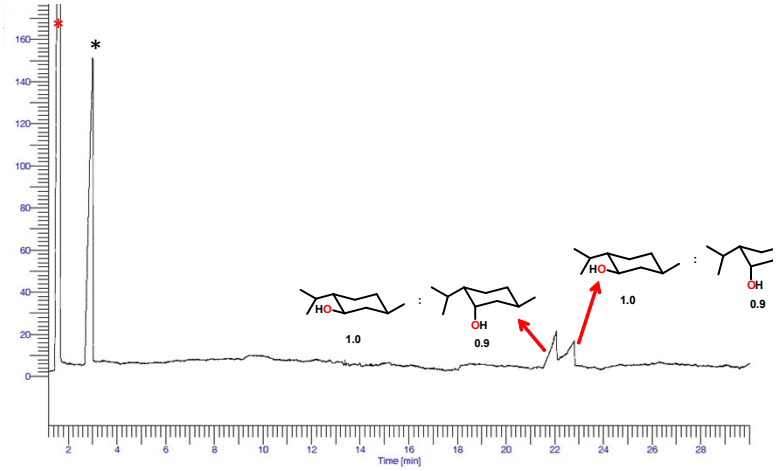

Figure S67. Gas chromatogram for the transfer hydrogenation of menthone, Scheme 2, Entry 2 using method B. * Represents ethyl acetate and * represents isopropanol.

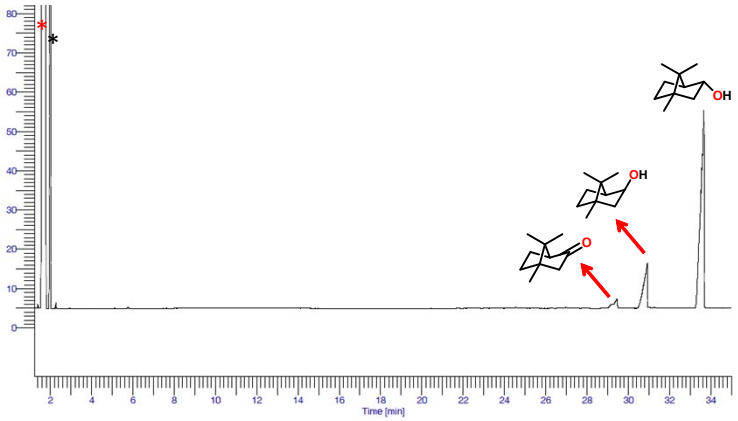

Figure S68. Gas chromatogram for the transfer hydrogenation of camphor, Scheme 2, Entry 3 using method B. * Represents ethyl acetate and * represents isopropanol.

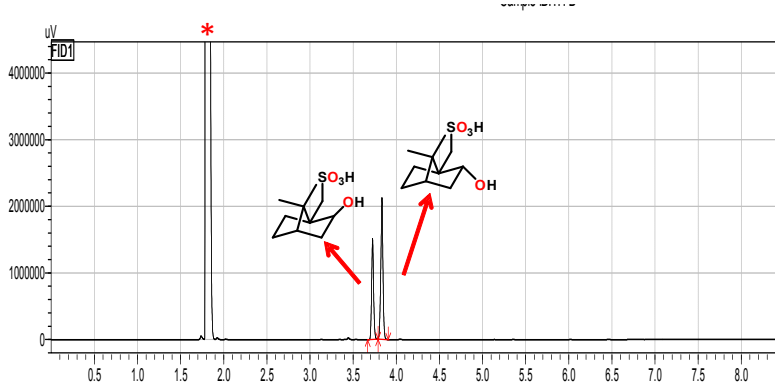

Figure S69. Gas chromatogram for the transfer hydrogenation of 10-camphorsulphonic acid, Scheme 2, Entry 4 using method C. * Represents ethyl acetate.

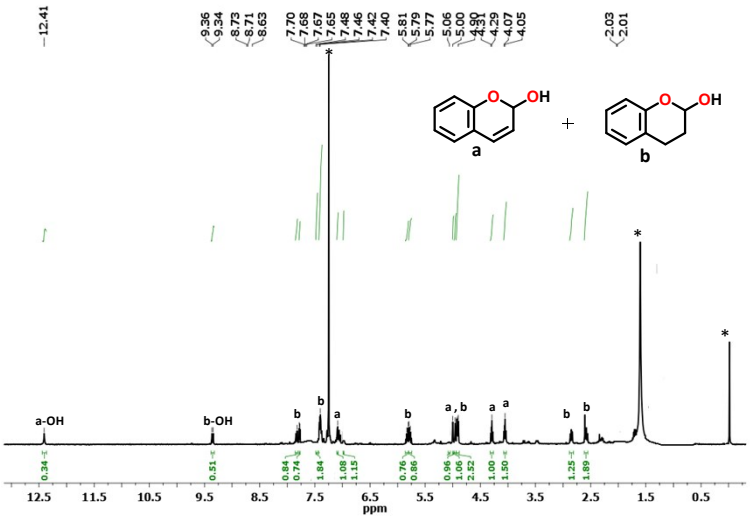

Figure S70. ^{1}H NMR spectrum of TH products of coumarin in $CDCl_3$. * Represents the residual solvent peak and/or water.

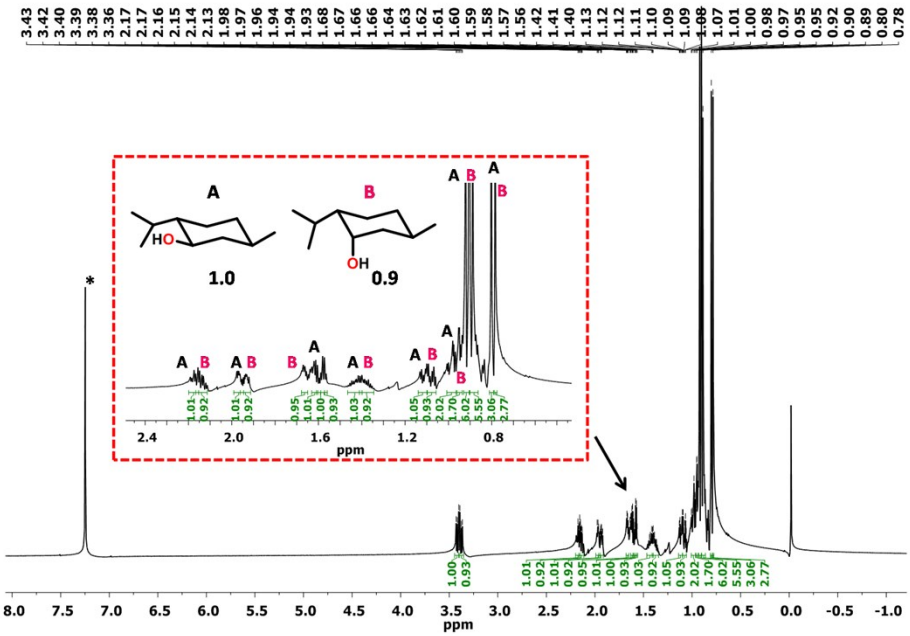

Figure S71. ^{1}H NMR spectrum of diastereomers of menthone in $CDCl_3$. * Represents the residual solvent peak.

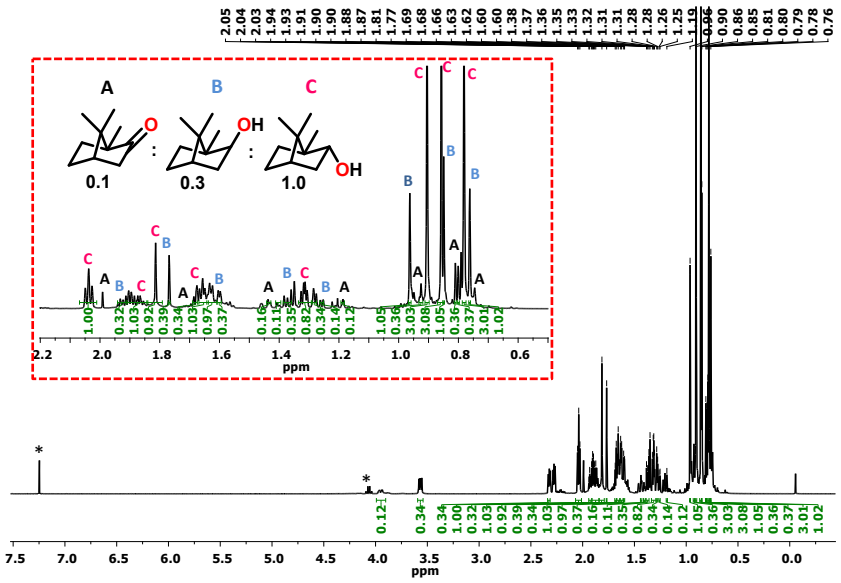

Figure S72. ^{1}H NMR spectrum of diastereomers of camphor in $CDCl_3$. * Represents the residual solvent peak.

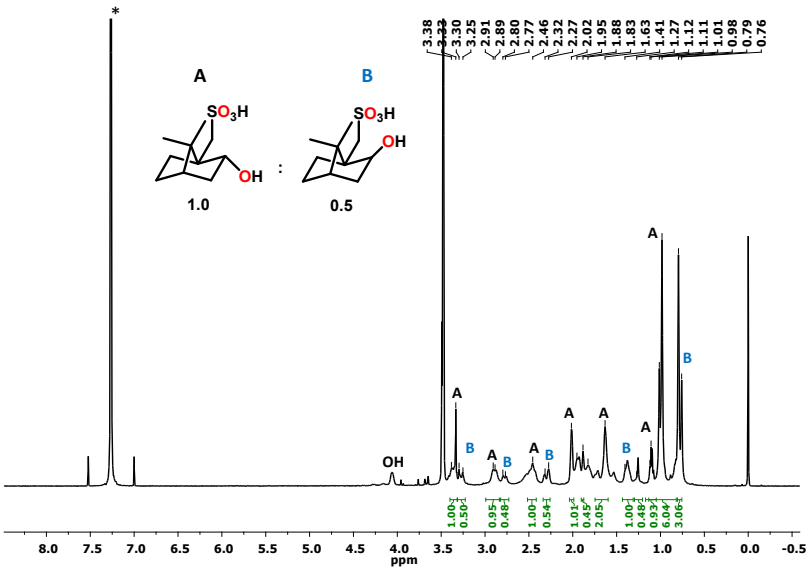

Figure S73. ^{1}H NMR spectrum of diastereomers of 10-camphorsulphonic acid in $CDCl_3$. * Represents the residual solvent peak.

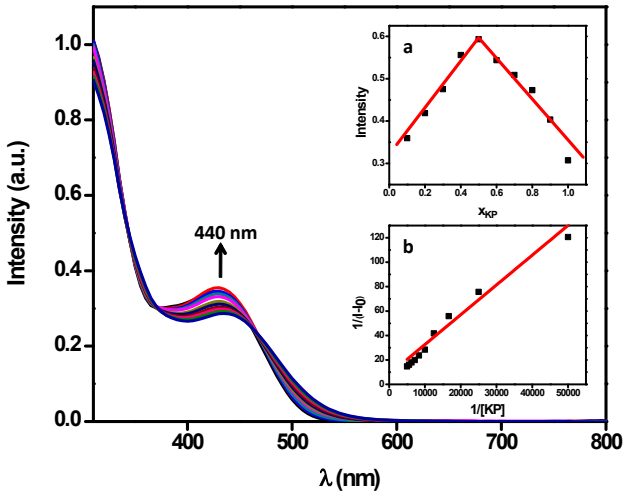

Figure S74. UV-Vis spectral titration of complex **3** (40 μM) with potassium isopropoxide in DMF. Inset **a**: Job's plot showing a 1:1 binding stoichiometry between complex **3** and isopropoxide ion. Inset **b**: Linear regression fitting curve for a 1:1 binding between complex **3** and isopropoxide ion.

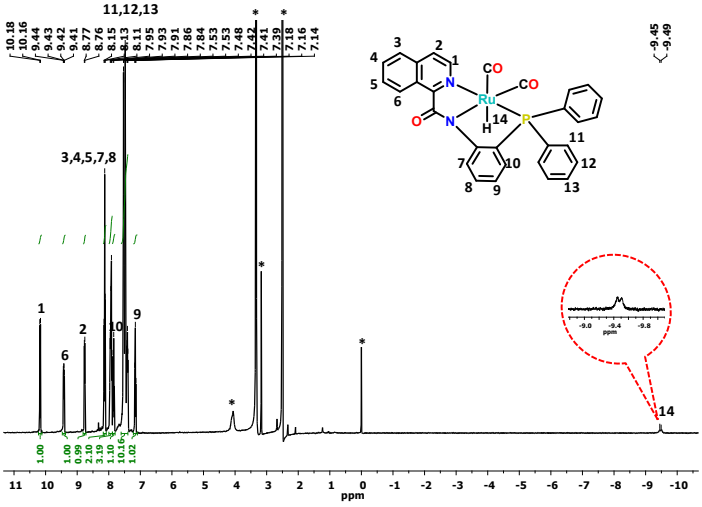

Figure S75. ^{1}H NMR spectrum of complex **4** in DMSO-d_6. * Represent residual solvent peaks.

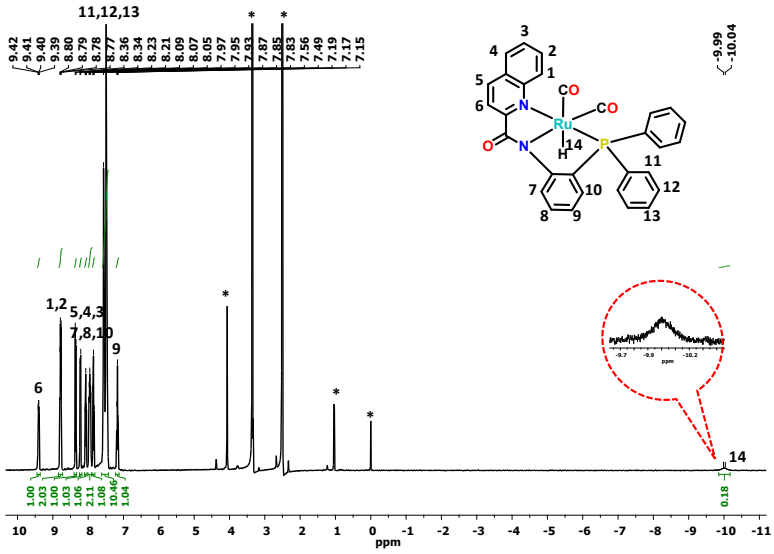

Figure S76. ^{1}H NMR spectrum of complex **5** in DMSO-d_6. * Represent residual solvent peaks.

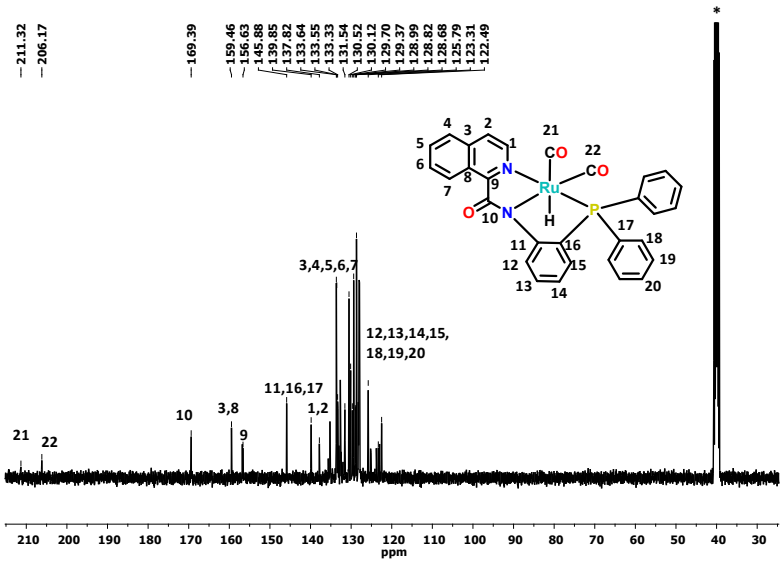

Figure S77. Selected part of ^{13}C NMR spectrum of complex **4** in DMSO-d_6. * Represents residual solvent peak.

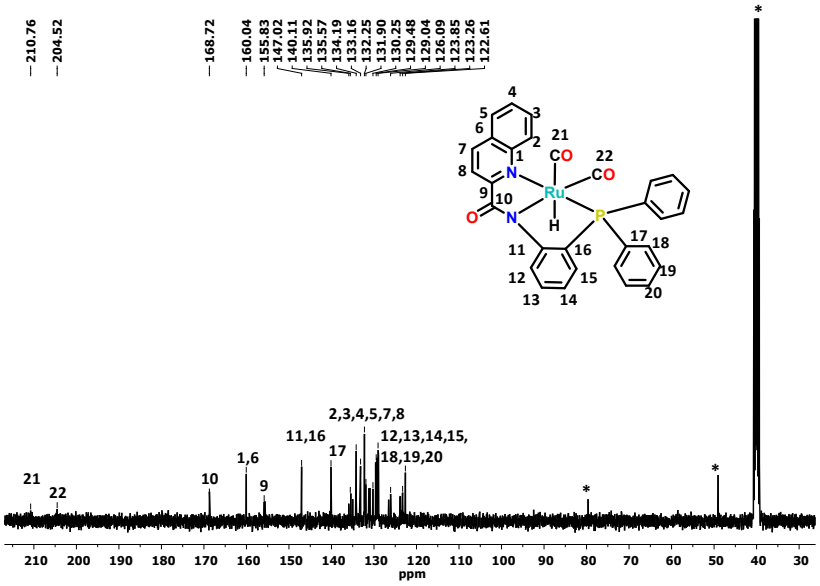

Figure S78. Selected part of ^{13}C NMR spectrum of complex **5** in DMSO-d_6. * Represents residual solvent peak.

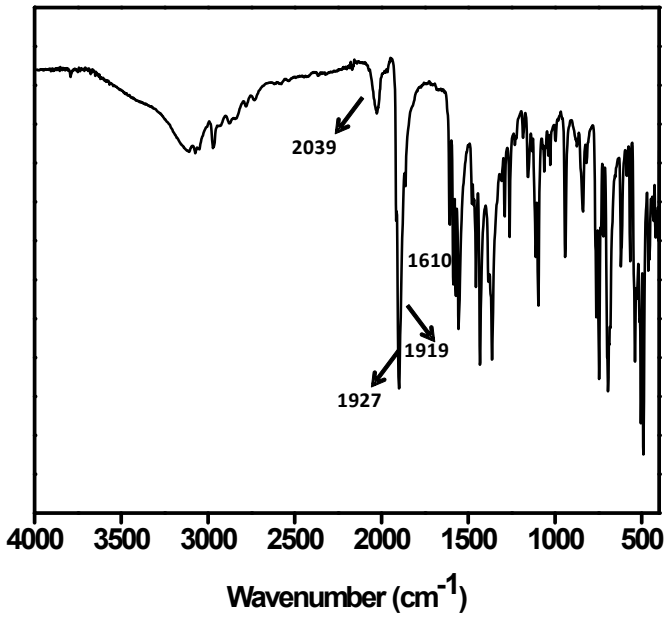

Figure S79. FTIR spectrum of complex **4**.

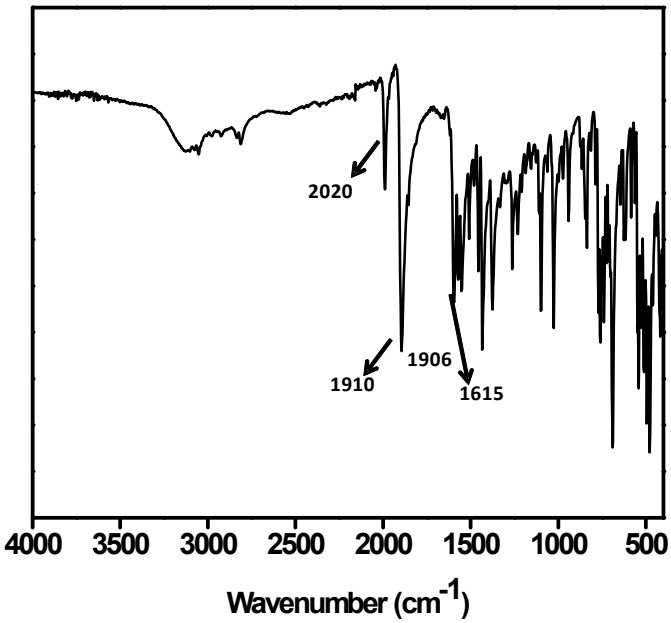

Figure S80. FTIR spectrum of complex **5**.

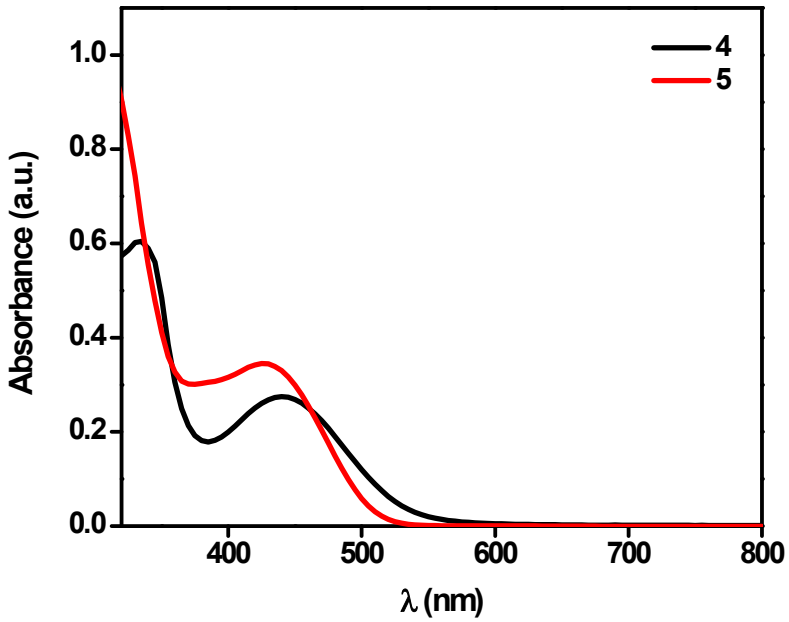

Figure S81. UV-Vis spectra of complexes **4** (black trace) and **5** (red trace) recorded in DMF.

^{1}H NMR spectra used for the calculation of yields for the Hammett plot:

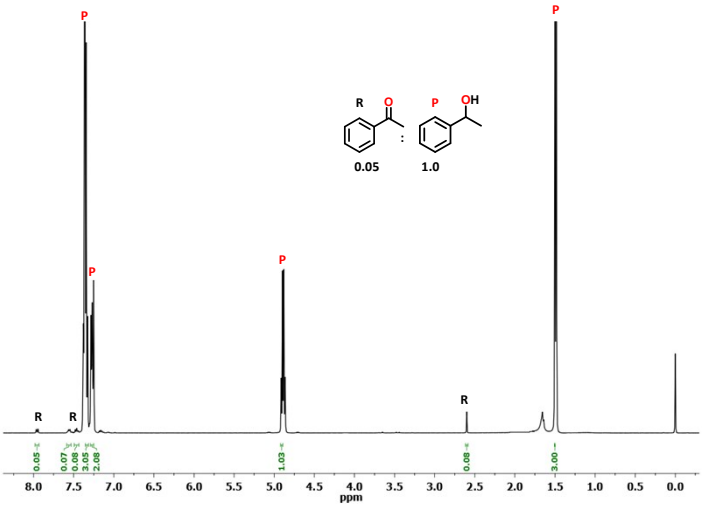

Figure S82. ^{1}H NMR spectrum of a reaction mixture for the TH of acetophenone in $CDCl_3$.

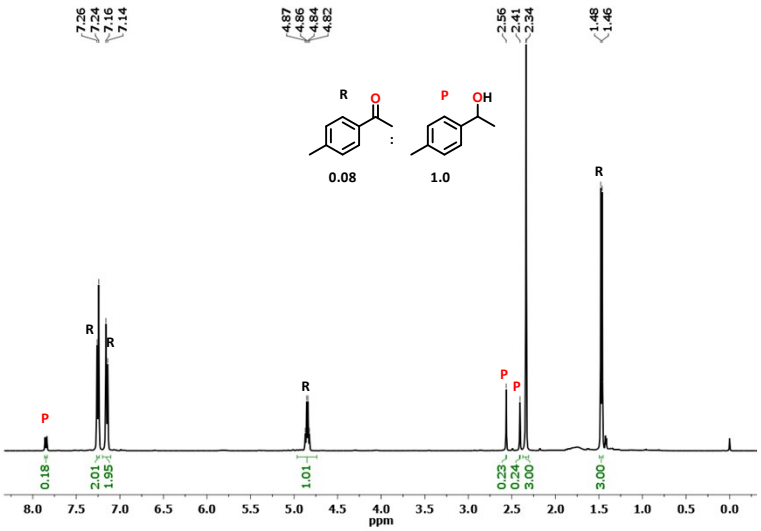

Figure S83. ^{1}H NMR spectrum of a reaction mixture for the TH of 4-methylacetophenone in $CDCl_3$.

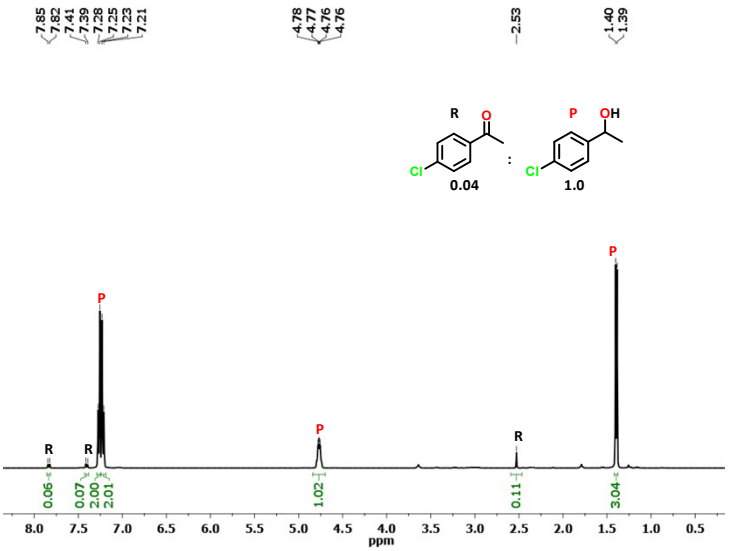

Figure S84. ^{1}H NMR spectrum of a reaction mixture for the TH of 4-chloroacetophenone in $CDCl_3$.

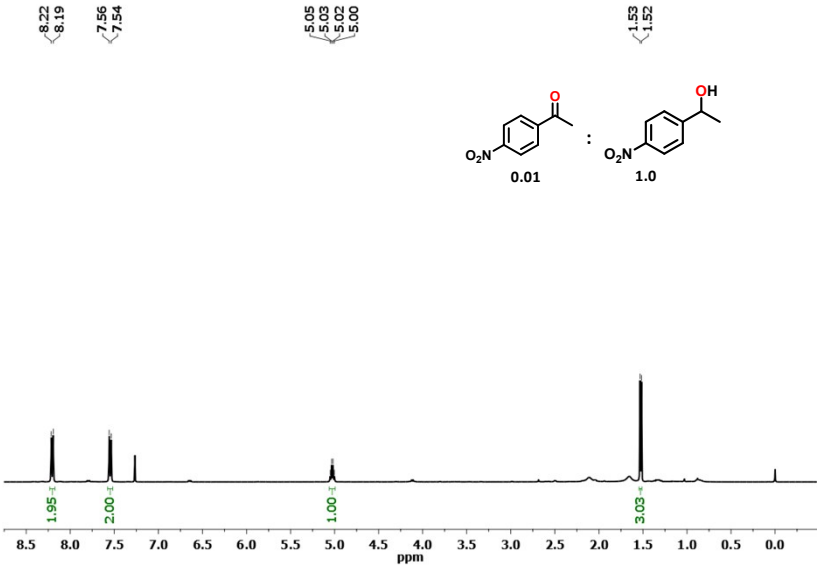

Figure S85. ^{1}H NMR spectrum of a reaction mixture for the TH of 4-nitroacetophenone in $CDCl_3$.

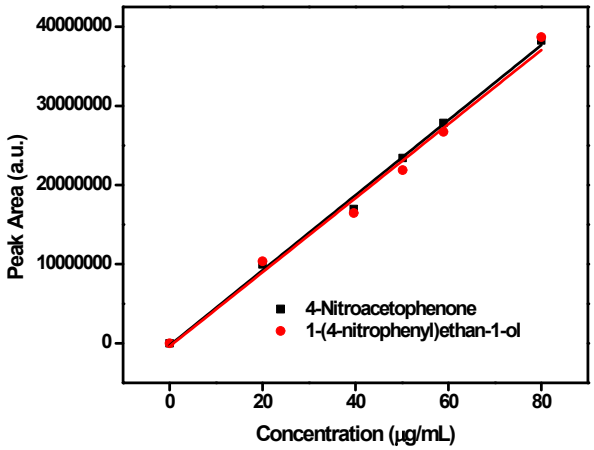

Figure S86. GC calibration plot for a mixture of 4-nitroacetophenone and 1-(4-nitrophenyl)ethan-1-ol).

Table S1. X-ray data collection and structure refinement parameters for complexes **1-3**.

	1	**2**	**3**
CCDC No.	**1993893**	**1993892**	**1993891**
Empirical formula	$C_{26}H_{22}ClN_2O_3PRu$	$C_{30}H_{20}ClN_2O_3PRu$	$C_{30}H_{20}ClN_2O_3PRu$
Formula weight	577.94	623.97	623.97
Temperature (K)	298(2)	298(2)	298(2)
Wavelength (Å)	0.71073	0.71073	0.71073
Crystal system	Monoclinic	Monoclinic	Triclinic
Space group	*I*2/a	$P2_1/n$	P$\bar{1}$
Unit cell dimensions			
a(Å)	18.3088(8)	8.6093(12)	9.9715(4)
b(Å)	8.4872(4)	19.520(2)	11.0618(4)
c(Å)	32.8245(16)	16.0093(18)	12.8149(4)
α°	90	90	92.082(3)
β°	101.520(4)	101.983(12)	98.606(3)
γ°	90	90	108.609(3)
Volume ($Å^3$)	4997.9(4)	2631.8(6)	1319.19(9)
Z	8	4	2
Density Mg/m3 (calculated)	1.536	1.575	1.571
Absorption coefficient mm^{-1}	0.829	0.794	0.792
F(000)	2336	1256	628
Crystal size (mm^3)	0.25 x 0.20 x 0.16	0.19 x 0.15 x 0.09	0.22 x 0.17 x 0.11
Theta range for data collection	3.278 to 29.612°	3.255 to 30.884°	3.498 to 24.999°
Index ranges	-25<=h<=25, -11<=k<=11, -45<=l<=45	-12<=h<=12, -28<=k<=28, 23<=l<=23	-11<=h<=11, -13<=k<=13, -15<=l<=15

Reflections collected	31483	38198	15256
Independent reflections	4384 [R(int) = 0.0556]	6858 [R(int) = 0.1200]	4637 [R(int) = 0.0259]
Completeness to theta = 25°	99.7 %	99.8 %	99.7 %
Refinement method	Full-matrix least-squares on F^2	Full-matrix least-squares on F^2	Full-matrix least-squares on F^2
Data / restraints / parameters	4384 / 0 / 311	6858 / 0 / 343	4637 / 0 / 343
Goodness of-fit on F^2	1.023	0.975	1.074
Final R indices [I>2sigma(I)]	R1 = 0.0364, wR2 = 0.0813	R1 = 0.1008, wR2 = 0.2211	R1 = 0.0237, wR2 = 0.0539
R indices (all data)	R1 = 0.0466, wR2 = 0.0859	R1 = 0.1840, wR2 = 0.3019	R1 = 0.0265, wR2 = 0.0553
Largest diff. peak and hole (e.Å^{-3})	0.641 and -0.376	1.727 and -1.552	0.281 and -0.291

$R1 = \Sigma||Fo| - |Fc||/\Sigma|Fo|$; $wR = \{\Sigma[w(Fo^2 - Fc^2)_2]/\Sigma[wFo_4]\}^{1/2}$

Table S2. Selected bond distances (Å) and bond angles for complexes **1-3**.

Bond Length (Å)	**1**	**2**	**3**
Ru(1)-C(1)	1.811(4)	1.890(10)	1.877(3)
Ru(1)-N(2)	2.068(3)	2.073(5)	2.088(16)
Ru(1)-N(1)	2.141(3)	2.112(6)	2.174(16)
Ru(1)-O(3)	2.183(2)	---------	---------
Ru(1)-P(1)	2.275(9)	2.292(2)	2.308(5)
Ru(1)-Cl(1)	2.408(10)	2.422(2)	2.416(6)
Ru(1)-C(2)	---------	1.895(8)	1.895(2)

Bond Angles (°)	**1**	**2**	**3**
C(1)-Ru(1)-N(2)	95.40(14)	92.6(4)	93.00(11)
C(1)-Ru(1)-N(1)	95.80(13)	92.2(3)	92.18(9)
N(2)-Ru(1)-N(1)	79.11(11)	174.5(3)	173.08(9)
C(1)-Ru(1)-O(3)	177.86(14)	89.0(3)	89.26(8)
N(2)-Ru(1)-O(3)	86.34(10)	105.0(3)	106.37(8)
N(1)-Ru(1)-O(3)	83.31(10)	77.7(2)	78.28(6)
C(1)-Ru(1)-P(1)	91.59(11)	89.7(3)	89.83(7)
N(2)-Ru(1)-P(1)	83.85(8)	94.5(3)	92.02(7)
N(1)-Ru(1)-P(1)	161.97(8)	82.89(17)	83.41(5)
O(3)-Ru(1)-P(1)	89.82(7)	160.45(15)	161.61(5)
C(1)-Ru(1)-Cl(1)	88.96(13)	175.1(2)	173.32(7)
N(2)-Ru(1)-Cl(1)	173.24(8)	88.8(3)	87.88(8)
N(1)-Ru(1)-Cl(1)	95.35(9)	86.60(18)	87.51(5)
O(3)-Ru(1)-Cl(1)	89.19(8)	86.1(2)	84.13(5)
P(1)-Ru(1)-Cl(1)	101.22(3)	94.87(7)	96.76(2)